Pharm Res (2015) 32:1161–1185
DOI 10.1007/s11095-014-1545-6

EXPERT REVIEW

Nanoparticles and the Blood-Brain Barrier: Advancing from *In-Vitro* Models Towards Therapeutic Significance

David J. Mc Carthy • Meenakshi Malhotra • Aoife M. O'Mahony • John F. Cryan • Caitriona M. O'Driscoll

Received: 17 July 2014 / Accepted: 6 October 2014 / Published online: 2 December 2014

ABSTRACT The blood-brain barrier is a unique cell-based restrictive barrier that prevents the entry of many substances, including most therapeutics, into the central nervous system. A wide range of nanoparticulate delivery systems have been investigated with the aim of targeting therapeutics (drugs, nucleic acids, proteins) to the brain following administration by various routes. This review provides a comprehensive description of the design and formulation of these nanoparticles including the rationale behind individual approaches. In addition, the ability of currently available *in-vitro* BBB models to accurately predict the *in-vivo* performance of targeted nanoparticles is critically assessed.

KEY WORDS Blood-brain barrier · Drug delivery to the CNS · *In vitro* models · Targeted nanoparticles · Transcytosis

Introduction

Neurological disorders are diseases that affect the central and peripheral nervous systems. According to the National Institute of Neurological Disorders and Stroke (NINDS) (1), there are more than 600 disorders that affect the nervous system ranging from neurodegenerative (Alzheimer's, Parkinson's, Amyotrophic lateral sclerosis, Huntington's) and cerebrovascular (brain tumours, stroke), to neuro-inflammation and neuro-infections (multiple sclerosis, herpes encephalitis, acquired immunodeficiency syndrome), all of which lead to degeneration of the affected area(s) of the central nervous system (CNS) and to psychiatric disorders such as schizophrenia, anxiety & depression. Moreover, epilepsy and autism are also common brain disorders and there is a host of rare, often genetic-based, neurological disorders representing a significant unmet medical need. Finally, brain cancers are among the most pernicious of all cancers. Most of these disorders are classified as incurable with poorly understood pathogenesis. It is estimated that 35.6 million people worldwide have dementia, with Alzheimer's disease being the most common cause (60–70% of the cases) (2). Neurodegenerative diseases, such as Alzheimer's and Parkinson's, not only have a significant impact on patient's health and cognitive function, but also lead to large global economic cost. This global economic burden is likely to increase further with an increasing elderly population (3–5).

To date, the availability of effective therapies for the majority of neurological diseases is extremely limited. These therapeutics can include nucleic acids (siRNA, DNA) (6, 7), proteins/peptides (8) and small molecules (usually chemotherapeutics) (9). The biggest challenge to such therapies lies in delivering the therapeutic compound to the targeted site i.e. the brain, as indicated by the failure of most developed biotherapeutics to access the brain in sufficient quantities (10). The two major limitations to drug delivery are transfer across the blood-brain barrier (BBB) and distribution and diffusion of the therapeutic to the intended target site. Most of the currently employed methods for treatment of neurological diseases are invasive, such as direct injection or infusion and, therefore, are associated with post-surgical complications. Thus, there exists an urgent need to design non-invasive, safe and effective drug delivery systems capable of efficient delivery to the CNS.

This review outlines the architecture and the materials used in the formulation of nanoparticle-based drug/gene delivery

David J. Mc Carthy and Meenakshi Malhotra have made an equal contribution

D. J. Mc Carthy • M. Malhotra • A. M. O'Mahony • C. M. O'Driscoll (✉)
Pharmacodelivery group, School of Pharmacy, Cavanagh Pharmacy Building, University College Cork, Cork, Ireland
e-mail: caitriona.odriscoll@ucc.ie

D. J. Mc Carthy • J. F. Cryan
Department of Anatomy and Neuroscience, Western Gateway Building University College Cork, Cork, Ireland

J. F. Cryan
Laboratory of Neurogastroenterology, Alimentary Pharmabiotic Centre Cork, Ireland

systems for targeted delivery to the brain. In addition, the ability of *in-vitro* BBB models to accurately predict the *in-vivo* performance of targeted nanoparticles is critically assessed.

Blood-brain Barrier

The BBB is a dynamic structure which effectively separates the CNS from the circulatory system and protects the CNS from potentially harmful chemicals, toxins and infection. It is formed by brain microvascular endothelial cells (BMECs) which line the microvessels of the brain, along with closely associated astrocytes and pericytes (11–13). Together, these cells form a functional "neurovascular unit" that maintains a highly selective permeable barrier and regulates the central blood flow (Fig. 1).

One integral feature of the BBB is the presence of tight junctions (TJs) between the adjacent BMECs. Tight junctions are formed from proteins including claudins (e.g. claudins 1 and 5), occludin and junction adhesion molecules, which are linked by cytoplasmic accessory proteins such as zonula-occludens and cingulin to the beta-actin cytoskeleton (14). Other molecules are also shown to be involved in the regulation of tight junctions e.g. annexin-1 (15). Together, these proteins span the gap between adjacent BMECs leading to the formation of a tight monolayer. The presence of TJ's reduces paracellular movement of substances and contributes to the high transendothelial electrical resistance (TEER) of >1,500 Ω cm^2 (16).

The selective permeability of the BBB mainly favours the transport of small, lipophilic compounds <400-500 Da, thereby limiting access of many therapeutics (17–19). Typically, these therapeutic compounds are large drug molecules (neuropeptides, antibiotics, anticancer and hydrophilic therapeutic agents), that cannot pass through the BBB and often, are substrates for the various efflux transporters and enzymes expressed by BMECs and are expelled back into the circulation (20). The presence of tight junctions, while allowing the passage of specific smaller drugs via paracellular movement, restricts the transcytosis of most solutes and macromolecules. Therefore, the major routes of transport for macromolecules across the BBB include carrier-mediated, receptor-mediated, adsorptive and fluid-phase endocytosis. Potential exists to exploit these routes for drug delivery.

- Carrier-mediated transport

  Carrier-mediated transport is facilitated by specific transport proteins that carry hydrophilic small molecules such as amino acids, nucleosides and glucose either from blood to brain or brain to blood. These carrier transport proteins are present on both luminal and abluminal surface of the capillary endothelium (21). This bidirectional movement of molecules across the BBB is catalysed by chemical/electrical gradients. Examples of carrier mediated transporters present at the BBB are glucose (GLUT1), lactate (MCT1), large neutral amino acid (LAT1) and adenosine (CNT2) transporters (22).
- Receptor-mediated transcytosis

  Receptor-mediated transcytosis is facilitated by receptors present on the luminal surface of the capillary endothelium, which leads to the endocytosis of the ligand bound to the receptor. This is followed by transport within endosomes/lysosomes or transcytosis across the cell interior and exocytosis from the abluminal surface of the capillary endothelium. Examples of proteins involved in receptor-

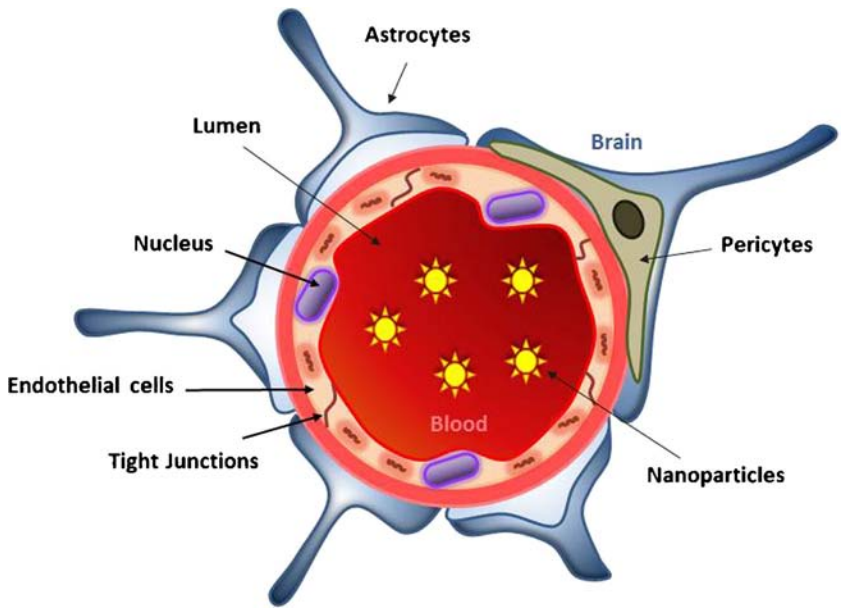

Fig. 1 Illustrative representation of the structure of the neurovascular unit of blood-brain barrier as it would appear *in-vivo*. The nanoparticles (shown in the lumen of the blood vessel) have to bypass the blood-brain barrier to enter the central nervous system.

mediated transport across the BBB include insulin, transferrin, low-density lipoproteins and leptin receptors (23).

- Adsorptive endocytosis

  Adsorptive endocytosis, like receptor mediated endocytosis, is a vesicle mediated method of transport. It requires a high charge on the macromolecule that enables non-specific interaction with the cell membrane e.g. cationised albumin (24, 25).
- Fluid-phase endocytosis

  Fluid phase endocytosis is another non-specific entry mechanism that arises from the invagination of the cell membrane to form a vesicle. The contents trapped in the fluid inside this vesicle is then internalised by the cell (25).

Adsorptive and receptor-mediated endocytosis are known to be the most common routes of entry across the BBB, as BMECs show reduced levels of fluid phase endocytosis compared to other cell types (25, 26).

Another transport mechanism that plays a significant role in limiting access of molecules into the CNS are the active efflux transporters, such as the ATP binding cassette transporters (ABC) (e.g. P-glycoprotein) present on the luminal surface of the endothelium. These efflux transporters and enzymes (e.g. cytochrome P450) complement the physical barrier of BMECs and tight junctions by forming a metabolic barrier that can degrade a variety of xenobiotics or eject them from the cell back into the blood (27, 28). In addition, efflux transporters (e.g. ASCT2, OAT3, NET) are present on the abluminal surface of the endothelium, which enable the clearance of neurotoxins and metabolites produced by the brain, in order to maintain the function of the CNS (29).

Together, the BMECs, TJs and efflux transporters act as a barrier that confers effective protection to the CNS, which is vital for maintaining the correct environment for neuronal function (22). However, in certain disease conditions, the integrity of the BBB is known to be disrupted and in such instances the BBB itself contributes to the disease pathology (28). For example, in Alzheimer's disease, stroke and CNS cancers, inflammation can affect the integrity and transport functions of the BBB. In such conditions, the BBB itself becomes a potential target for therapeutics (20, 24, 30, 31).

Drugs can be administered to the brain by invasive routes (direct injection/infusion) or non-invasive routes (such as systemic). Currently, most clinical drug-delivery strategies rely on invasive surgical interventions that involve mechanical breach of the BBB to deliver therapeutics. Such strategies present a greater risk to patient health, lack patient acceptability and are costly. In addition, these strategies are limited to local delivery, which may not be beneficial for diseases like Alzheimer's or multiple sclerosis, where multiple sites within the CNS may be affected. Thus, there exists a need to develop systemic drug delivery approaches that have the ability to efficiently transport drug across the BBB, leading to its widespread distribution across the entire brain parenchyma in therapeutically relevant quantities.

Nanotechnology for Therapeutic Delivery to the CNS

Nanotechnology offers exciting prospects and great potential with regards to CNS drug delivery, by overcoming some of the limitations of conventional drug delivery approaches. Nanocarriers are colloidal systems ranging from 1 to 300 nm in size and include a range of materials such as natural or synthetic polymeric nanoparticles, solid lipid nanoparticles, dendrimers, cyclodextrins, micelles, gold nanoparticles and carbon nanotubes (32–34) (Fig. 2). These colloidal particles carry an active therapeutic agent (drug, gene, protein, vaccine), which may be adsorbed, dissolved, encapsulated, covalently attached or electrostatically bound to the particle (35). We have previously reviewed the formulation and application of non-viral nanosystems for gene delivery to the CNS (34). An ideal nanocarrier for CNS drug delivery is one which offers efficient delivery across the BBB with selective targeting, protects the therapeutic cargo from enzymatic degradation. In addition, it achieves long circulation time, enables self-regulated drug release, prevents efflux transport, has low immunogenicity, good biocompatibility and bioavailability (36, 37). A key advantage of loading therapeutics into the nanoparticles for brain delivery is the potential to achieve a high drug concentration in the brain parenchyma of a drug that otherwise has poor distribution. These colloidal particles are amenable to modifications on their surface by various other molecules, such as surfactants or coating agents, that contribute to membrane fluidisation or inhibition of the transmembrane efflux transporters (P-glycoprotein) respectively (37), thereby facilitating cellular uptake of nanoparticles.

Uptake of nanoparticles is dependent on physicochemical characteristics, such as size and surface charge. Size exerts significant impact on the mechanism of uptake, whereby particles of <200 nm in size tend to be internalised by clathrin-mediated endocytosis, while larger particles (~500 nm) are generally internalised by caveolae-mediated endocytosis (38). Various investigations have shown the effect of nanoparticle size on distribution to brain, with higher concentrations of small nanoparticles (10–50 nm) tending to accumulate in the brain tissue compared to nanoparticles of >200 nm in size (39, 40). Ultra-small nanoparticles are susceptible to clearance by hepatic filtration when administered systemically, but this can be minimised by administration via the intranasal route through inhalation or as intranasal drops. Intranasal administration, has potential to deliver nanoparticles directly to the brain either via the olfactory, trigeminal or paracellular pathway, bypassing the blood brain barrier and minimizing the risk of systemic exposure (41–43). Another

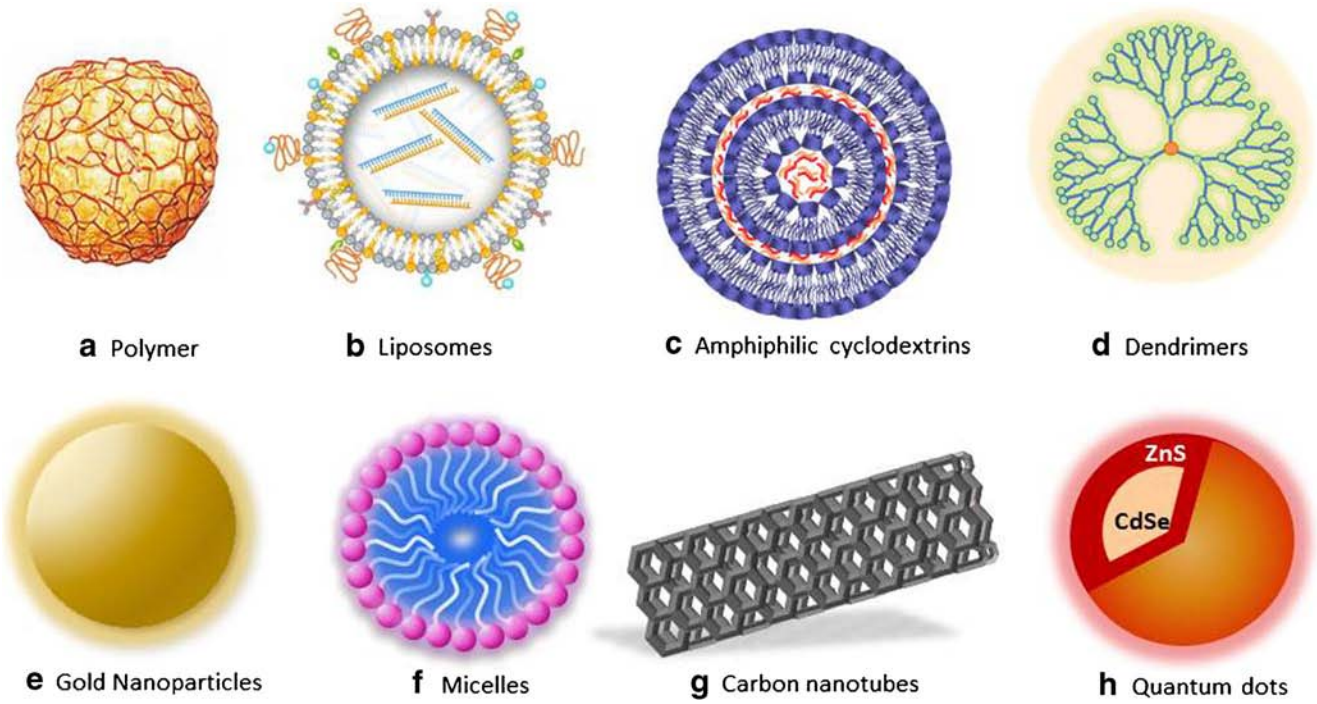

Fig. 2 Different types of nanoparticles commonly used for biomedical applications and which offer significant potential in delivering therapeutics across the blood-brain barrier.

method being investigated is the temporary disruption of the BBB by microbubble enhanced unfocused ultrasound (44). This has been utilised to greatly increase the entry of PEG-PLGA nanoparticles functionalised with the 6E10 antibody (anti amyloid-beta) (44).

In addition to size, the surface charge and surface properties of nanoparticles further affect the uptake and transcytosis *in-vivo*. Enhanced cellular uptake of nanoformulations has been observed in the case of cationic nanoparticles, as they interact with the negatively charged cell membrane and undergo adsorptive-mediated endocytosis, while neutral or negatively charged nanoparticles tend to be internalised only if they are tagged with a ligand that interacts with a cell-specific receptor (45). However, a disadvantage of cationic nanoparticles is their tendency to interact non-specifically with various proteins in the blood stream leading to the formation of "corona" (which refers to the adsorption of opsonins on the nanoparticles surface) (46). This can result in undesirable effects such as complement activation and blood clotting. In addition, such opsonized nanoparticles are rapidly cleared from the circulation via the reticuloendothelial system (RES).

The most common approach of evading RES uptake is to coat the nanoparticle with a neutral, hydrophilic polymer such as polyethylene glycol (PEG) or with polysorbates, yielding nanoparticles with "stealth" properties and with resulting prolonged circulation time and enhanced stability in the circulation (47). The conferred neutral surface charge of 'stealth' nanoparticles limits their cellular uptake; however, they can be further modified with cell-specific ligands to mediate active targeting via the transport systems present on the surface of the cell membrane.

Various ligands can be employed for targeting including peptides such as Rabies Virus Glycoprotein (RVG) (48) or macromolecules such as transferrin (49), insulin (50), folate (51) and monoclonal antibodies (52). Such a receptor-mediated approach to transfer across the BBB has been pioneered by Pardridge and co-workers, who reported successful delivery of a variety of nucleic acid cargoes into the brain after intravenous administration of insulin or transferrin antibody-conjugated PEGylated liposomal formulations (53, 54). One potential drawback to the use of antibodies as targeting ligands is their large molecular weight which increases the overall size of the nanoparticles and may, therefore, be a hindrance to biodistribution/spreading in the brain parenchyma. However, an attempt has been made to use Fab (fragment antigen binding) domains instead of the entire antibody. The Fab region provides specificity to the antibody. This technique not only reduces the overall molecular weight of the binding entity but also reduces immunogenicity by impeding various functions such as phagocytosis, complement activation and antibody-dependent cellular cytotoxicity (55).

The following section describes the range of nanoparticle systems under investigation for therapeutic delivery to CNS and includes comprehensive information on the materials

Table I Nanoformulations Used for Delivery of Therapeutics to the Brain

Nanoparticle type	Nanoformulation	Targeting ligand	Cargo	*In vitro* BBB model	*In vivo* model	Reference
Gold nanoparticles						
	Gold nps	Not used	Not used	Primary rat BMEC	Not used	(181)
	Gold nps	THR-CLPFFD peptide	Not used	Primary Bovine BMEC	Rat	(143)
	Gold nps	HSA or Tf	Not used	hCMEC/D3	Not used	(182)
	Gallium-68 coated gold nps	Enk neuropeptide	Not used	Not used	Rat	(183)
	Gold nps	Insulin	Not used	Not used	Rat and mouse	(50)
Micelles						
	Triton X 100 and Lutensol AP 20 micelles	Not used	Kynurencic acid	Primary Rat BMEC	Rat	(138)
	Polymeric micelles	Not used	C6 coumarin	MDCK	Not used	(172)
Cyclodextrins						
	Amphiphilic cyclodextrin	Not used	HTT siRNA	Not used	R6/2 HD mouse	(94)
	Quaternary Ammonium β-Cyclodextrin	Not used	Doxorubicin	Primary Bovine BMEC	Not used	(142)
	β-cyclodextrin	Lactoferrin	IR-775 chloride dye	Not used	Mouse	(87)
Polymer						
	PHDCA	Polysorbate 80, PEG, Poloxamine 908	Fluobrite	Not used	Rat	(135)
	PEG-PHDCA nps	Not used	Not used	Primary rat BMEC	Not used	(134)
	PBCA	Polysorbate-80 coating	Cisplatin	Not used	C6 Glioma Rat	(184)
	PBCA	Polysorbate-80 coating	Doxorubicin	Not used	Rat	(185)
	PBCA	CRM 197	Zidovudine	Primary human BMEC	Not used	(186)
	Poly(L-lactide)	Not used	Flurbiprofen	bEnd.3	Not used	(187)
	PEG-PLGA	Not used	Loperamide	Caco-2	Mouse	(173)
	PLGA-PEG-PLGA	Polxamer 188 or polysorbate 80 coating	Loperamide	RBE4	Mouse	(188)
	PLGA	BSA, Tf	Not used	Not used	F98 glioma rat	(189)
	PLGA	5 novel peptides	Not used	Not used	Rat	(190)
	Modified PLGA	Not used	Not used	Not used	Rat	(191)
	PEG-PTMC nps	2-deoxy-D-glucose	Paclitaxel	bEnd.3	Rg-2 glioma mouse	(192)
	DGL	Dermorphin	shRNA	Not used	Mouse	(193)
	DGL-PEG	Leptin 30	DNA	b.End3	Mouse	(7)
	Protamine-oligonucleotide nanoparticles	ApoA-I	Not used	Primary Porcine BMEC	Not used	(194)
	PLG	Polysorbate-80 coating	TIMP-1 protein	Primary rat BMEC and RBE4	Mouse	(195)
	PEG-PCL nps	AS1411 and TGN	Docetaxel	bEnd.3	U87 glioma mouse	(196)
Dendrimers						
	G4 PAMAM nps	Transferrin and Tamoxifen	Doxirubicin	Primary mouse BMEC	Not used	(9)
	G4 PAMAM nps	Biotinylated and non-biotinylated	Not used	Primary rat	Rat	(197)
	G4 and G4-C12 PAMAM nps	Not used	Not used	Not used	Mouse	(85)
Lipid nanoparticles						
	Liposomes	Wheat germ agglutinin and Tamoxifen	Topotecan	Species not mentioned	C6 glioma rat	(198)
	Liposomes	Tf and Tamoxifen	Epirubicin	Primary rat BMEC	C6 glioma rat	(139)
	Liposomes	Glucose	Coumarin-6	Primary rat BMEC	Mouse	(199)
	Liposomes	Tf and MAN	Danorubicin	Primary mouse BMEC	Rat	(200)

Table I (continued)

Nanoparticle type	Nanoformulation	Targeting ligand	Cargo	*In vitro* BBB model	*In vivo* model	Reference
	Solid lipid	83-14 MAb	Saquinavir	Primary human BMEC	Not used	(153)
	Fluorescent magneto liposomes	Tf	Not used	Primary human BMEC	Not used	(201)
	Immunoliposomes	Aβ-MAb	Not used	hCMEC/D3	Not used	(202)
	Liposomes	RI7217 MAb	Not used	hCMEC/D3	Not used	(163)
	Immunoliposomes	OX-26 MAb	Not used	hCMEC/D3	Not used	(162)
	Lipid	83-14 MAb	Carmustine	Primary human BMEC	Not used	(154)
	Immunoliposomes	ApoE	Curcumin	hCMEC/D3	Not used	(203)
	Liposomes	RMP-7	Nerve Growth Factor	Primary mouse BMEC	Rat	(141)
Metal oxide nanoparticles						
	TiO2 nps	Not used	Not used	Primary rat BMEC	Not used	(204)
	PEG-Fe3O4	Lactoferrin	Not used	Primary Porcine BMEC	Rat	(152)
	SiO2	Not used	Not used	hCMEC/D3	Not used	(164)
	Iron oxide nps	Anti PECAM-1	Not used	hCMEC/D3	Rat	(165)
	Superparamagnetic iron oxide nps	Not used	Not used	hBMEC	Not used	(205)
	PEGylated Silica nps	Not used	Not used	bEnd.3	Mouse	(206)
Quantum dots						
	Quantum rods	Tf	Not used	Primary human BMEC	Not used	(107)
	Quantum Dots	Not used	siRNA (MMP-9)	Primary human BMEC	Not used	(105)
	Silica nps and Quantum Dots	Not used	Not used	Primary rat BMEC	Not used	(207)
Albumin nanoparticles						
	HSA	HI 6 dimethanesulfonate and HI 6 dichloride monohydrate	Not used	Primary Porcine BMEC	Not used	(208)
	PEGylated HSA	ApoE	Oximes	Primary Porcine BMEC	Not used	(159)
Magnetic nanoparticles						
	Fe_3O_4	Not used	BDNF	Primary human BMEC	Not used	(209)
	Magnetic silica PLGA	Tf	Doxorubicin and Paclitaxel	Not used	U87 MG-luc2 mouse model	(49)
	MMA-SPM nps	RMP-7	Stavudine, Delavirdine and Saquinavir	Primary human BMEC	Not used	(210)
Carbon nanotube						
	Oxidised multi-wall carbon nanotube	Angiopep-2	Doxorubicin	Not used	C6 glioma mouse	(211)

BMECs Brain Microvascular Endothelial Cells, *HSA* Human Serum Albumin, *BSA* Bovine Serum Albumin, *Tf* Transferrin, *PEG* Polyethylene glycol, *ApoE* Apolipoprotein E, *nps* nanoparticles, *MAb* Monoclonal antibody, *BSA* Bovine Serum Albumin, *PBCA* Poly(butylcyanoacrylate), *PLGA* Poly(lactic-co-glycolic acid), *PAMAM* Polyamidoamine, *PHDCA* Poly(hexadecylcyanoacrylate), *DGL* Dendrigraft poly-l-lysine

used to fabricate NPs (Fig. 2), the targeting ligands and therapeutic cargos, as summarised in Table I.

Lipids

Liposomes

Liposomes consist of an aqueous core surrounded by one or more concentric phospholipid bilayers and have been widely investigated for systemic delivery of therapeutics. The common constituents that form part of phospholipid bilayer are sphingomyelin, phosphatidylcholine, and glycerophospholipids (47). Liposomes vary in size from small (<100 nm) and large (>100 nm) unilamellar vesicles, to multilamellar vesicles (>500 nm). Surface functionalized liposomes have been investigated for CNS delivery. For example, systemic delivery of 5-fluorouracil (5-FU) to the brain was reported using transferrin conjugated liposomes (56). The

results indicated a 17-fold increase in the uptake of the transferrin conjugated liposomes compared to free 5-FU by brain capillary endothelial cells in albino rats (56). In another approach, glutathione-targeted PEGylated liposomes were used to intravenously deliver methylprednisolone in a rat model of multiple sclerosis with acute experimental autoimmune encephalomyelitis (EAE). The results indicated an increase in plasma circulation and brain uptake of methylprednisolone in comparison to untargeted, PEGylated liposomes and methylprednisolone controls. In addition, a significant reduction in the clinical signs of the disease were reported compared to the control animals (57). Another similar study published the delivery of an opioid peptide DAMGO using glutathione-targeted PEGylated liposomes. The results indicated an increase in the half-life and higher brain exposure of the drug in comparison to controls (8). Ligands for LDL receptors on the brain have also been investigated for CNS delivery of liposomes. For example, angiopeptide (a ligand for low-density lipoprotein receptor-related protein (LRP1), expressed on the BBB) conjugated liposomes were used to deliver the chemotheraputic drug mitoxantrone to the brain, resulting in a significant reduction in the tumour size in a mouse model (58).

Further modifications to liposomes have also been investigated to enhance their suitability for biomedical application, as outlined below.

Cationic Liposomes

Cationic liposomes self-assemble in the presence of nucleic acids to form "lipoplexes", due to the electrostatic interaction between the positively charged lipids and the negatively charged phosphate groups on DNA/RNA and have been extensively investigated for gene delivery (59). The most commonly used cationic lipids include 1,2-dioleoyl-3-trimethylammonium-propane (DOTAP) and 1,2-Dioleoyl-sn-glycero-3-phosphocholine (DOPC). These cationic lipids are often mixed with a helper lipid, such as dioleoylphosphatidylethanolamine (DOPE). DOPE is a neutral phospholipid which undergoes structural changes at acidic pH, leading to increased endosomal release (60). Cationic liposomes are internalised by adsorptive-mediated endocytosis, followed by destabilization of the endosomal membrane at pH 5–6. Examples of brain delivery include lactoferrin modified procationic liposomes which were shown to cross brain endothelial cells *in-vitro* (61) and cationic polymeric magnetic liposomes (20 nm), which delivered paclitaxel to the brain in rats after intra-arterial administration (62).

Solid Lipid Nanoparticles (SLN)

Unlike liposomes, solid-lipid nanoparticles have a hydrophobic core, which is advantageous in dispersing hydrophobic drugs. They are usually composed of triglycerides, fatty acids and waxes (63). They are prepared by various methods including hot/cold homogenization and microemulsification (63). Solid lipid nanoparticles have shown great promise over other polymeric nanoparticles, in terms of their scalability, lower toxicity, higher drug loading capacity and controlled release over longer time periods, however, their application is limited to encapsulation of hydrophobic drugs only (64). A recent study showed increased uptake of fluorescently labelled camptothecin solid lipid nanoparticles (<200 nm) into the rat brain after systemic administration (65). Surface modification of solid lipid nanoparticles to improve their specificity for the brain has been reported. For example, polysorbate 80, which promotes adsorption of apolipoprotein E to the nanoparticle surface, enhanced uptake of solid lipid nanoparticles into the brain after intravenous injection (66). Apolipoprotein E is taken up by low density lipoprotein (LDL) receptors on BMECs.

A search of the clinicaltrials.gov website shows three clinical trials involving liposomal formulations for delivery to the brain including a phase 1 trial to assess delivery of CPT-11 liposomes to treat recurrent high grade glioma (67), a phase two trial to treat cerebral lymphoma B with a combination of PEGylated liposomal doxorubicin and dexamethasone (68) and the use of rhemium nanoliposomes to treat recurrent glioblastoma (69).

Polymeric Micelles

Polymeric micelles are amphiphilic copolymers with A (hydrophilic)-B (hydrophobic) diblock structures. They form stable spheroidal structures in aqueous media with a hydrophobic [polypropylene glycol, poly (D, L-lactide), poly (caprolactone)] core and hydrophilic (polyethylene glycol) surface. They range in size from 10 to 100 nm and can be designed to release the entrapped drug in response to pH, temperature, light or ultrasound (70). Pluronic type block copolymers are composed of ethylene oxide and propylene oxide. Enhanced delivery of digoxin, a P-glycoprotein substrate, in pluronic P85 nanoparticles both *in-vitro* and *in-vivo*, has been shown, due to the inhibition of the P-glycoprotein mediated efflux system (71). A recent study by Kim *et al.* reported successful delivery of beta-galactosidase protein to the brain in rabies virus glycoprotein (RVG) conjugated chitosan-Pluronic nanoparticles (72).

Polymeric Nanoparticles

Polymeric nanoparticles are prepared from natural or synthetic materials such as poly(butylcyanoacrylates) (PBCA), poly(methylidene malonate), polyesters (poly(lactic acid) (PLA), poly(lactic-co-glycolic acid) (PLGA), poly(ε-caprolactone)), amino acids (poly(aspartic acid), poly(lysine)), polysaccharides (chitosan,

cyclodextrin, alginate), or proteins (gelatine, albumin) (73). Most polymeric nanoparticles are biodegradable and biocompatible and are readily functionalised with ligands or other polymers, due the availability of reactive functional groups. Poly(butylcyanoacrylates) (PBCA) nanoparticles functionalized with polysorbate 80, containing a compound, dalargin, an endorphin that possesses opioid activity, were readily taken up by the brain endothelial cells via LDL receptors, thereby increasing the analgesic effect induced by the compound (74). PBCA nanoparticles have also been used to deliver other conventional drugs, such as (methotrexate, doxorubicin, temozolomide) (75–77), and nucleic acids such as, antisense molecules and plasmids (78). However, the use of PBCA nanoparticles has been limited due to the toxic hydrolysis by-products (polycyanoacrylic acid and alcohol). On the contrary, polyester polymers such as PLGA and PLA are preferred for brain drug delivery studies as their autocatalytic hydrolysis yields non-toxic oligomers of lactic and glycolic acid, which are degraded to CO_2 and H_2O. These polyester nanoparticles have achieved increased concentration of dexamethasone and vasoactive intestinal peptide in the brain (79, 80). A recent study showed that systemic delivery of stable PLGA nanoparticles with entrapped antituberculosis drugs (rifampicin, isoniazid, pyrazinamide, and ethambutol) achieved sustained drug levels in the brain *in-vivo* (81).

Nanoparticles derived from natural materials such as starch are often preferred over synthetic materials for their biodegradability and lack of or low toxicity e.g. chitosan. Recently, chitosan nanoparticles and their derivatives have been extensively investigated for intranasal delivery of therapeutics (siRNA, neuropeptides and drugs) to target the brain (42, 82, 83). Intranasal administration of siRNA using modified chitosan nanoparticles (size <20 nm), conjugated with a TAT peptide (a cell penetrating peptide) and a MGF peptide (a cell targeting peptide) resulted in brain delivery of the siRNA 4 h later, specifically targeting the hippocampus, thalamus, hypothalamus, and Purkinje cells (41).

Dendrimers

Dendrimers are composed of repetitive units of branched molecules and form a 3-dimensional spheroidal shape in aqueous media. With extended branching around the periphery, the dendrimers form radially crowded layers. Thus, the core is loosely packed in comparison to the periphery and is suitable for the entrapment of drugs (84). The most commonly used polymers for the formation of dendrimers are poly(amidoamine) (PAMAM) and poly(propylene imine). A very recent study showed the distribution characteristics of PAMAM dendrimers in brain tissues, after intraparenchymal and intraventricular injection, depended on the surface functionalisation (85). Another study looking at size-dependent uptake showed that, after systemic administration, functionalized PAMAM dendrimers of <12 nm traversed the BBB by the paracellular route and reached RG-2 malignant gliomas (40). Another study showed that PAMAM dendrimers accumulated in the microglia and astrocytes of the brain tissues of rabbits with cerebral palsy, delivering N-acetyl-L-cysteine, an anti-inflammatory agent for the treatment of neuro-inflammatory disorders (86).

Cyclodextrins

Cyclodextrins are another example of naturally derived materials which have been explored for their ability to deliver therapeutic payloads across the BBB (87, 88). Cyclodextrins are cone shaped, with hydrophilic primary and secondary faces and a hydrophobic cavity. Cyclodextrins can be modified by various functional groups due to the presence of hydroxyls on their primary and secondary faces, yielding a whole range of amphiphilic, cationic, PEGylated and targeted molecules (89–93). We recently reported efficient delivery of siRNA by a cationic amphiphilic β-cyclodextrin in both *in-vitro* and *in-vivo* models of Huntington's disease (94). These nanoparticles were found to be stable in cerebrospinal fluid and achieved a significant reduction in the expression of the HTT gene in the striatum after local administration of the nanoformulation, with little or no toxicity (94, 95).

Gold

Gold nanoparticle formulations are generally colloidal suspensions of particles in aqueous solution. They are inert and non-toxic to cells and have previously been used for imaging due to their ability to absorb and scatter near-infrared light (96). A biodistribution study conducted by Sonavane *et al.* demonstrated size dependent uptake of systemically delivered gold nanoparticles in mouse brain tissue after 24 h, with 500 fold higher uptake of 15 nm gold nanoparticles compared to 100 nm nanoparticles (97). However, the concentration in the tissue with 100 nm gold nanoparticles was only 30% lower than nanoparticles of 15 nm in size. Gold nanoparticles can also be utilised for the delivery of nucleic acids for gene silencing. Direct injection of gold nanorods complexed with GAPDH siRNA was shown to elicit long term gene knockdown (11 days) in the rat hippocampus with a single injection (98). Ultrafine-gold nanoparticles in size range 1–50 nm have been shown to cross intestinal barriers after oral administration and to target secondary organs, such as the brain, opening up other routes for brain delivery (39, 99).

Carbon and Inorganic Materials

Inorganic materials such as titania, alumina, silica and iron have gained much popularity in imaging and diagnostic

studies and are now being explored for drug delivery applications. These nanoparticles are of stable size and form monodisperse suspensions, which is an advantage over polymeric nanoparticles. Drug loaded silica nanoparticles are formed by mixing the silica shell with drug, wherein the drug coalesces on the surface of the silica matrix on drying. Silica nanoparticles can be modified with various functional groups, such as amines for interaction with nucleic acids, without any apparent cyto/neurotoxicity (100). A labelled silica nanoparticle tracer for diagnosis and imaging in melanoma and malignant brain tumour patients is currently in clinical trial (101); this formulation had previously shown good toxicity and targeting in mice (102).

Carbon nanotubes and fullerenes have also been used for drug/gene delivery. Solid ultrafine carbon nanoparticles of 36 nm size were reported to target the CNS, when administered by inhalation, with the authors concluding that airborne nanoparticles of this size can access the CNS from the olfactory mucosa via the olfactory nerve (42). However, their use is limited due to their capacity to induce lipid peroxidation and generate free radicals that can lead to toxicity (103).

Quantum Dots

Quantum dots are another class of inorganic nanomaterials, characterized as colloidal semi-conductor nanocrystals ranging from 2 to 50 nm in size. They have been used previously for diagnostic purposes (fluorescent probes) as well as functionalised for delivery of therapeutics (104, 105). As fluorescent probes, they show long fluorescence lifetime and photostability in comparison with other fluorescent dyes and proteins (106). Quantum dots have also been investigated *in-vitro* for delivery of the anti-retroviral drug Saquinavir to treat HIV-1 in the CNS and MMP-9 siRNA to improve BBB integrity (107).

Cell Penetrating/Targeting Peptides

Cell penetrating peptides have gained much interest owing to their ability to translocate across biological membranes. Cell penetrating peptides are protein transduction domains that consist of positively charged amino-acid sequences, typically less than 20 amino acids in length, mainly consisting of arginine and lysine. The arginines and lysines can interact with the negatively charged head groups present on the cell membrane, such as heparan sulfate, sialic or phospholipidic acid (108–111), allowing diffusion across the cell membrane and delivery of the therapeutic payload directly into the cytoplasm. Cell penetrating peptides such as penetratin and transportan have been used to conjugate siRNA and enhance its cellular uptake (112). Other cationic peptides that have been used for gene delivery are MPG (27-mer peptide) (113) and cholesteryl oligo-D-arginine (Chol-R9) (114). Different routes of endocytosis have been proposed for cell penetrating peptides, including caveolae (115), macropinocytosis (116, 117), through a clathrin-dependent pathway (118), via a cholesterol-dependent clathrin-mediated pathway or in the trans-Golgi network (118). Direct translocations via lipid membrane (119) and energy independent pathways (120, 121) have also been reported. Cell penetrating peptide-mediated nanoparticle delivery was first reported using the transactivator-of-transcription (TAT) peptide conjugated to iron oxide nanoparticles (40 nm) *in vivo* (121). TAT is a basic peptide (RKKRRQRRR) derived from the transduction domain of HIV-1 (108). The iron oxide particles modified with TAT peptide resulted in approximately 100-fold higher uptake efficiency in lymphocytes compared to the unmodified particles.

Other than cell penetrating peptides, cell targeting peptides have also been used for brain targeting. Cell targeting peptides are ligands that show high specificity and affinity towards a specific receptor that is exclusively over expressed by a particular cell. RGD peptide, a ligand for the integrin ($\alpha v\beta 3$) receptor, has been the most extensively studied cell targeting peptide (122). Angiopeps are peptides developed by Angiochem, which have the ability to transport therapeutics across the BBB via LRP1 receptors present on the brain endothelial cells. Specifically, ANG1005 is an angiopep-2 peptide conjugated with 3 molecules of paclitaxel and has shown enhanced uptake (10 to 100 fold) of the drug in the brain parenchyma (123, 124). These peptides offer advantages over the use of antibodies, due to their small size and efficient cell targeting.

Although a number of systemically administered nanoparticles have been used to target the CNS, most studies involve local administration of the nanoformulation. Local administration limits the clinical acceptability of nanoparticles as a delivery approach. An ideal nanoparticle delivery system should be capable of crossing the BBB following administration by non-invasive means. Intranasal and other routes of delivery are being explored, however, clinical translation of such technologies and patient compliance are challenging. Thus, systemic administration still remains the most likely method of successfully delivering therapeutics across the brain in the clinic. The ability to accurately evaluate transfer across the BBB and subsequent release of the therapeutic payload in the targeted cells is the most important criteria for assessing nanoparticles. Due to the expense of testing nanoformulations *in-vivo*, much of the initial work on nanoparticle formulation is conducted *in-vitro* in relevant cell models, e.g. endothelial cells, neuronal cells, glial cells. Several research studies have employed combinations of cell types (co-cultures) to mimic the *in-vivo* properties of BBB. The following section details the advantages and limitations of the various *in-vitro* BBB models currently used and critically evaluates their ability to accurately predict the *in-vivo* delivery potential of nanoparticles.

Table II List of Cell-Based Blood–Brain Barrier Models Used to Screen Various Nano-Drug Formulations

Cell model	Species	Cargo	Nanoformulation	TEER ($\Omega.cm^2$)	Membrane permeability (cm/s)	Reference
RAT						
Primary BMECs	Rat	N.G.	Gold	N.G.	[NaFlu] = 1.61 ± 0.11 × 10^{-6}	(181)
Primary BMECs and asts	Both rat	6-Coumarin	BSA and Cationic BSA conjugated PEG-PLA	313 ± 23	[^{14}C] = 0.96 × 10^{-3}	(212)
Primary BMECs and asts	Both rat	Kynurencic acid	Triton X 100 and Lutensol AP 20 micelles	320 ± 37	2.28 ± 0.4 × 10^{-6}	(138)
Primary BMECs and asts	Both rat	N.G.	PEG-PHDCA	>250 for both co and monoculture	[^{14}C] = 1.86 ± 0.18 × 10^{-6} [^{3}H] = 1.38 ± 0.36 × 10^{-6}	(134)
Primary BMECs and asts	Both rat	N.G.	N.G.	>600	N.G.	(213))
Primary BMECs and asts	Both rat	N.G.	TiO_2	Not given	[^{14}C] = 4.15 ± 0.96 × 10^{-6}	(204)
Primary BMECs, Asts and Pericytes	All rat	N.G.	N.G.	354 ± 15	[NaFlu] = 4 × 10^{-6}	(127)
Primary BMECs, Asts and Pericytes	All rat	N.G.	Silica and quantum dots	150-300	N.G.	(207)
MOUSE						
Primary BMECs	Mouse	Doxirubicin	Tf and Tamoxifen functionalized G4PAMAM	>250	N.G.	(9)
Primary BMECs	Mouse	Danorubicin	Tf and MAN functionalized liposome	>250	N.G.	(200)
Primary BMECs	Mouse	DNA	Leptin30 functionalized DGL-PEG	N.G.	N.G	(7)
Primary BMECs	Mouse	NGF	Liposome	~200	N.G.	(141)
Primary BMECs	Mouse	N.G	Lactoferrin modified PAMAM	200	N.G.	(214)
PORCINE						
Primary BMECs	Porcine	N.G.	N.G.	Serum- 400 Serum free- 700	Serum- [^{14}C] = 4.5 ± 0.6 × 10^{-6} Serum Free- [^{14}C] = 1.0 ± 0.4 × 10^{-6}	(146)
Primary BMECs	Porcine	N.G.	N.G.	~800	[^{14}C] = 3 × 10^{-6}	(215)
Primary BMECs	Porcine	N.G.	Obidoxime functionalized HSA	N.G.	N.G.	(208)
Primary BMECs	Porcine	N.G.	PEG-Fe_3O_4 conjuagted to lactoferrin	>700	N.G.	(152)
Primary BMECs	Porcine	Oximes	PEGylated or ApoE modified HSA	~700	N.G.	(151)
Primary BMECs and astrocytes	Both Porcine	N.G.	ApoA-I coated protmaine-oligonucleotide	590 ± 125	[^{14}C] = 1.21.2 × 1010^{-6}	(194)
BOVINE						
Primary BMECs	Bovine	Doxorubicin	Quaternary Ammonium β-Cyclodextrin	156.4 ± 0.65	[LY] = ~2.7 × 10^{-5} [FD4k] = 8.2 ± 0.7 × 10^{-6}	(142)
Primary BMECs	Bovine	N.G.	Emulsifying wax/Brij 78 and Brij 72/ Tween 80 nps	N.G.	[^{14}C] = 8.6 ± 0.43 × 10^{-4}	(216)

Table II (continued)

Cell model	Species	Cargo	Nanoformulation	TEER ($\Omega.cm^2$)	Membrane permeability (cm/s)	Reference
Primary BMECs and asts	Bovine		Tween®20, BSA and transferrin coated PLGA	N.G.	$[^{14}C] = < 1.6 \times 10^{-5}$	(217)
Primary BMECs and asts	Bovine BMEC and rat asts	N.G.	THR-CLPFFD conjugated gold nanoparticles	141 ± 3.31	$[LY] = 9.6 \pm 1.9 \times 10^{-6}$	(143)
Primary BMECs and asts	Bovine BMECs and Rat asts	N.G.	N.G.	857 ± 39 (highest value)	$[FD4k] = 1.5 \pm 0.7 \times 10^{-6}$	(144)
Primary BMECs and asts	Bovine BMECs and rat asts	Dalargin	Polysorbate-80 coated poly(butylcyanoacrylate)	N.G.	$[^{14}C] = 3.1 \pm 0.2 \times 10^{-3}$	(218)
HUMAN						
Primary BMECs	Human	N.G.	N.G.	>1000 Ω	N.G.	(132)
Primary BMECs and asts	Both Human	N.G.	Tf conjugated quantum rods	120.1 ± 5.72 to 126.6 ± 3.31	N.G.	(107)
Primary BMECs and asts	Both Human	N.G	Quantum Dots	~250 $\Omega.cm^2$	N.G.	(105)
Primary BMECs and asts	Both Human	N.G.	N.G.	~700 with flow ~100 static	$[^{14}C] = 2.9 \times 10^{-7}$	(174)
Primary BMECs and asts	Both Human	BDNF	Magnetic nps	287.6 ± 9.4	N.G.	(209)
Primary BMECs and asts	Both human	Saquinavir	83-14 MAb functionalized solid lipid	~220	N.G.	(153)
Primary BMECs and asts	Both human	N.G.	Tf functionalized Fluorescent Fe3O4 liposomes	~200	N.G.	(201)
Primary BMECs and asts	Both human	Zidovudine	CRM197 functionalized PBCA	N.G.	N.G.	(186)
Primary BMECs and asts	Both human	Stavudine, Delavirdine and Saquinavir	RMP7-MMA-SPM	N.G.	N.G.	(210)
Primary BMECs and asts	Both human	Carmustine	83-14 MAb functionalized solid lipid	237	N.G.	(154)
STEM CELLS						
IMR90-4 and primary astrocytes	Human BMECs and rat asts	N.G.	N.G.	$1,450 \pm 150$	$[^{14}C] = 5.7 \times 10^{-7}$	(169)
hCMEC/D3						
hCMEC/D3	Human BMECs	N.G.	Gold and TiO_2	40-50	N.G.	(182)
hCMEC/D3	Human BMECs	N.G.	Aβ-MAb functionalized immunoliposome	60 ± 8.9	$[LY] = 2.45 \times 10^{-7}$	(202)
hCMEC/D3	Human BMECs	N.G.	RI7217 MAb functionalised liposome	123 ± 6	$[^{14}C] = 2.47\ 10^{-7}$ $[^{3}H] = 5.85 \times 10^{-7}$	(163)
hCMEC/D3	Human BMECs	N.G.	SiO_2	40	$[FD4k] = \sim 3.5 \times 10^{-6}$ and $\sim 5 \times 10^{-6}$	(164)
hCMEC/D3	Human BMECs	N.G.	N.G.	30-40	$[^{14}C] = 1.65 \pm 3 \times 10^{-6}$ $[^{3}H] = 0.36 \pm 5 \times 10^{-7}$	(130)
hCMEC/D3	Human BMECs	N.G.	OX-26 MAb conjugated immunoliposomes	63.9 ± 5.5 (with simvastatin)	$[LY] = 2.3 \pm 0.081 \times 10^{-5}$	(162)
hCMEC/D3	Human BMECs	N.G	Anti-PECAM-1 conjugated Iron oxide	>90	$[LY] = 2.9 \pm 0.081 \times 10^{-6}$	(165)
hBMEC						
hBMEC	Human BMECs	N.G.	Superparamagnetic iron oxide	43.3 ± 0.44	N.G.	(205)

Table II (continued)

Cell model	Species	Cargo	Nanoformulation	TEER ($\Omega.cm^2$)	Membrane permeability (cm/s)	Reference
RBE4						
RBE4	Rat BMECs	Curcumin	ApoE conjugated immunoliposomes	45.1 ± 3.8	$[^{14}C] = 1.33 \times 10^{-5}$	(203)
RBE4 and C6	Both Rat	Loperamide	Poloxamer 188 or polysorbate 80 modified PLGA-PEG-PLGA nps	N.G.	N.G.	(188)
b. End3						
bEnd.3	Mouse BMECs	N.G.	Quaternary ammonium β-cyclodextrins	23.6 ± 2.7	$[NaFlu] = \sim 9 \times 10^{-6}$	(160)
bEnd.3 and RG-2	Mouse BMECs and Rat glioma	Paclitaxel	2-deoxy-D-glucose -PEG-PTMC	>200	N.G.	(192)
bEnd.3 and U87	Mouse BMECs and human glioblastoma	Doxorubicin and Paclitaxel	Iron oxide-mesoporous silica-PLGA	>250	N.G.	(49)
bEnd.3 and C6	Mouse BMECs and Rat asts	Docetaxel	AS1411 and TGN modified PEG-PCL	>150	N.G.	(196)
bEnd.3	Mouse BMECs	N.G	PEGylated Silica	>300	N.G.	(206)
bEnd.3	Mouse BMECs	Flurbiprofen	Poly(L-lactide)	~40	N.G.	(187)
b.End3 and C6 astrocytes	Mouse (b.End3) and Rat (C6)	N.G.	N.G.	bEnd3 alone = 40, bEnd3 + C6 = 80, bEnd3 + C6 + cAMP elevators = 130	bEnd3 alone = 19.4×10^{-6}, bEnd3/C6 = 19.4×10^{-6}, bEnd3/C6 + cAMP = 16.4×10^{-6}	(157)
b.End3 and CD81A	Both mouse	N.G.	N.G.	Co-culture with flow = ~270	Co-culture with flow $[FD4k] = \sim 7 \times 10^{-5}$	(175)
cEnd						
cEnd	Mouse	N.G.	N.G.	900-1,000	N.G.	(129)
CACO-2						
Caco-2	Human epithelial	Loperamide	PEG-PLGA	1,500	N.G.	(173)
MDCK						
MDCK	Canine epithelial	C6 coumarin	Polymeric micelle	>250	N.G.	(172)

BMEC Brain Microvascular Endothelial Cells, *asts* astrocytes, [*NaFlu*] sodium fluorescein, [*LY*] Lucifer yellow, [*FD4k*] FITC Dextran Mw 4,000, [*14C*] 14C sucrose, [*3H*] 3H propranolol. *HSA* Human Serum Albumin, *BSA* Bovine Serum Albumin, *Tf* Transferrin, *PEG* Polyethylene glycol, *MAb* Monoclonal antibody, *PBCA* Poly(butylcyanoacrylate), *PLGA* Poly(lactic-co-glycolic acid), *PHDCA* Poly(hexadecylcyanoacrylate), *PAMAM* Polyamidoamine, *DGL* Dendrigraft poly-l-lysine, *N.G.* Not Given

In-Vitro Blood-Brain Barrier Models—the Ability to Predict *in Vivo* Performance of Nanoparticle Delivery Systems

In-vitro models of the BBB have become essential as a tool to determine the ability of nanoparticles to deliver therapeutic cargoes across the BBB, enabling identification and evaluation of the optimal formulations for *in vivo* studies. Table II details a comprehensive list of cell types used to create *in-vitro* BBB models and examples of the various nanoparticle formulations tested in these models.

An ideal *in-vitro* BBB model is expected to resemble the *in-vivo* environment as closely as possible, i.e. restrictive paracellular pathway, *in-vivo* like cell morphology, expression of BBB specific transporters and efflux proteins (125). Unfortunately, due to the complexity of the BBB, the *in-vitro* models

currently used in research are far from ideal and there is a need for improved models which maintain a balance between the complexity of the system, ease of development and use.

The majority of these *in-vitro* BBB models use transwell inserts, which contribute to ease of use. Transwell inserts are commercially available in a range of sizes, materials and membrane pore size. A membrane pore size of 0.4 to 3 μm is generally used for drug transport studies. The simplest form of transwell model consists of a monoculture of BMECs cultured on the upper surface of the insert. However, in order to more closely mimic the *in-vivo* characteristics of BBB, a second cell type, such as astrocytes, can be co-cultured in the lower compartment either in contact (grown on the underside of the membrane) or non-contact (grown at the bottom of the lower compartment), as represented in Fig. 3. Co-culture of astrocytes in the lower compartment has been shown to improve the tightness of *in vitro* BBB models (126). Other cells that are co-cultured with BMECs include pericytes and neuronal cells (127). The simplicity of *in-vitro* transwell BBB models lends itself to high-throughput screening of nanoparticles and facilitates rapid optimization of experimental conditions (128). However, there are certain drawbacks to the use of transwell models, including the 2-dimensional architecture of the cells and the lack of a simulated blood flow (128). When compared to the neurovascular unit (Fig. 1), the transwell model lacks the complexity and cell-cell interactions that modulate the *in-vivo* BBB.

The tightness of a BBB model is determined by the TEER and the paracellular permeability. The TEER is a measure of the electrical resistance of the monolayer (Ohms.cm^2) and is determined by an ohmmeter. The paracellular permeability is determined by adding BBB impermeable tracer substances to the apical chamber of the transwell model and periodically measuring concentration found in the basolateral chamber. Concentrations are usually measured with HPLC (sucrose) or fluorescence (FITC dextran). A high TEER and low paracellular permeability is desirable (125, 126).

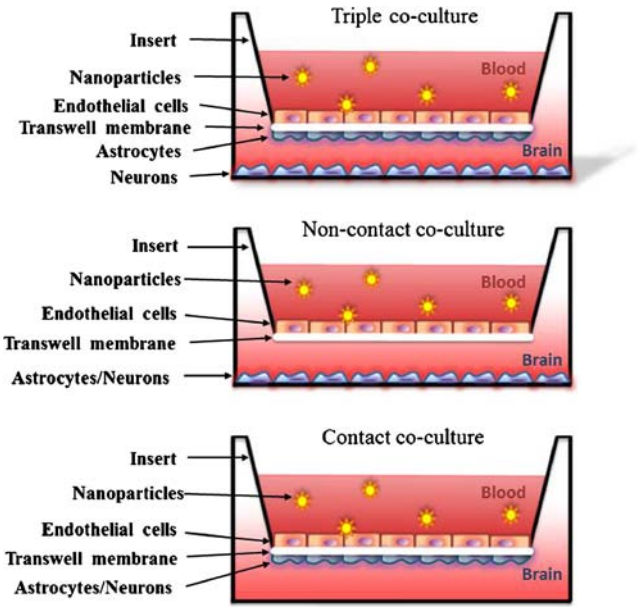

Fig. 3 Schematic representation of *in-vitro* transwell blood-brain barrier models. This represents (**a**) triple co-culture and (**b**) non-contact and (**c**) contact co-culture with astrocytes and neurons.

A wide range of cell types have been employed in *in vitro* BBB models. BMECs, used to mimic the brain capillary endothelium, are either derived from primary endothelial cells, isolated from the microvessels of the brain of different species, or endothelial cell lines, which have been immortalised through various techniques including the use of polyoma middle T oncogene (129), human telomerase and SV40 large T antigen (130). The following sections describe the various cell-based *in vitro* BBB models together with an evaluation of the ability of such models to predict *in vivo* performance.

Brain Endothelial Cells: Primary Cell Models

Primary cells are preferred for studying BBB integrity as they possess high TEER values with restrictive paracellular permeability and express various receptors and enzymes, similar to the *in-vivo* conditions (125). Primary endothelial cells can be obtained from various species including rat, mice, pigs, cows and humans. However, their procurement from the neurovascular unit is a challenging task, i.e. the cells need to be separated without being contaminated with other brain cells such as neurons, pericytes and astrocytes. The use of primary cells is limited to a short period of time, as they do not maintain their BBB characteristics for long (sub-culturing is limited to a few passages) and, in addition, they tend to exhibit batch to batch variability.

The procedure of isolating brain microvascular endothelial cells (BMECs) from the animal brain usually involves the removal of cortex, maceration, followed by multiple digestion steps and puromycin treatment to select a pure culture, which is then seeded onto the membranes to grow into a restrictive monolayer. This procedure involves intensive work and effort in procuring the cells, yet the yield obtained at the end is usually low. Significant efforts have been made to optimise and streamline the process in order to create improved primary cell models (131–133).

Rat

Primary brain endothelial cells derived from rat brains have been extensively used in research. Rats are widely used as *in-vivo* models, which facilitates *in-vitro* and *in-vivo* testing in the same rat strain (131). In culture, rat BMEC monolayers have shown specific characteristics of endothelial cells, such as expression of tight junction proteins (ZO-1, claudin-5, occludin, von Willebrand factor), transporters (P-gp, GLUT-1) and receptors (transferrin, LDL) (134). However, harvesting

cells from rat brains can be time consuming, and result in a low yield of cells. The cultured monolayer can be quite leaky and may eventually de-differentiate, losing its basic characteristics. A co-culture model formed with rat BMECs and astrocytes helps to maintain the BBB features and is more suitable for nanoparticle screening.

The transcytosis of PHDCA (Poly(hexadecylcyanoacrylate)) and PEGylated PHDCA nanoparticles was investigated using a co-culture model of primary rat endothelial cells and astrocytes (134). The model showed low paracellular permeability to sucrose (1.72×10^{-6} cm/s) and insulin (1.28×10^{-6} cm/s) and a TEER of 220–300 $\Omega.cm^2$, indicating that the monolayer was reasonably impermeable (134). However, TEER values, permeability and longevity in culture were improved by co-culture with astrocytes leading to increased expression of tight junction proteins. The transcytosis of the PEG-PHDCA nanoparticles across the monolayer was three fold greater compared to the non-PEGylated after 4 h, although this accounted for only 6 percent of the total dose (130). These results were in accordance with the *in-vivo* data from a previous study, which showed higher uptake of PEG-PHDCA nanoparticles in the brains of mice and rats compared to PHDCA nanoparticles alone, or coated in polysorbate 80 or poloxamine 908 (135).

Further work was undertaken by this group to elucidate the uptake mechanism of the PEG-PHDCA nanoparticles in primary rat endothelial cells (136). The addition of uptake inhibitors and pre-incubation of the PEGylated PHDCA nanoparticles with ApoE and ApoB-100, indicated the involvement of the low-density lipoprotein receptor in nanoparticle uptake (136, 137).

A recent study on kynurenic acid solubilised in non-ionic surfactants (Triton X-100 and Lutensol AP 20) showed a greater far permeability coefficient through the *in-vitro* rat BBB model relative to free kynurenic acid (free kynurenic acid $=11.58\pm0.3\times10^{-6}$ cm/s, Triton X-100 $=74.86\pm2.1\times10^{-6}$ cm/s, Lutensol $=164.45\pm14.14\times10^{-6}$ cm/s) (138). A comparative *in vivo* study following intraperitoneal injection in rats confirmed the *in vitro* results (138).

In another study, liposomes were modified to incorporate tamoxifen (to inhibit MDRs in the glioma cells) and transferrin (to target the BBB and glioma cells) (139). In the primary rat *in-vitro* BBB model the tamoxifen-transferrin liposomes showed the greatest transport after 24 h, as well as greater inhibition of C6 cell growth in a co-culture model. *In-vivo*, glioma rat models treated with the tamoxifen-transferrin liposomes also demonstrated the highest uptake in the brain and reduction in tumour volume resulting in increased survival rates relative to controls (139).

Murine

Primary murine brain endothelial cells (mouse BMECs) have also been widely used as BBB models and are particularly useful due to the availability of a multitude of transgenic mouse models for various disease conditions. The major limitation associated with murine BMECs is the low yield of endothelial cells procured from the mouse brain (approximately 1–2 million cells) and, therefore, a large number of animals must be sarcificed for high-throughput studies. Mouse BMECs have been shown to express the characteristic tight junction proteins and transporters along with leptin, transferrin and nicotinic acetylcholine receptors (140). This model can generate TEER values in the range 200–250 $\Omega.cm^2$ (9, 141).

A primary mouse cell model was used to investigate the uptake, transcytosis and toxicity of PAMAM nanoparticles, functionalised with RVG29 peptide, for targeted delivery of luciferase DNA to the brain via the nicotinic acetylcholine receptors (140). A significant increase in the permeability of RVG functionalised PAMAM:DNA nanoparticles through the BBB model was observed compared to non-targeted nanoparticles, without affecting the integrity of the cell monolayer (140). This finding correlated with the *in-vivo* studies, in which an increased amount of luciferase DNA expression was seen in the brains of mice treated with RVG-PEG:PAMAM:DNA nanoparticles (741 light units/mg protein) in comparison to the untargeted nanoparticles (431 light units/mg protein for PEG:PEMAM:DNA) after systemic injection (140). The untargeted nanoparticles were more effective in the *in vivo* study than may have been anticipated from the *in vitro* where they showed only ~33% of the uptake seen in the RVG functionalised nanoparticles.

Bovine

Isolation of bovine endothelial cells from calf brain can yield around 40 million cells per brain, which is approximately 10 times more than the yield from a mouse or a rat. The model is well characterized and expresses a variety of endothelial receptors, enzymes and transporters (125). These endothelial cell cultures are at times supplemented with cAMP elevators to strengthen the tight junctions, yielding high TEER values. Primary bovine BMECs cultured alone and without cAMP elevators yield TEER values between 100 and 200 $\Omega.cm^2$ (142, 143). However, when co-cultured with astrocytes and with the addition of cAMP elevators, a large increase in TEER values was reported (1,640 $\Omega.cm^2$), as well as decreased paracellular permeability of 0.48×10^6 cm/s (144). Bovine BMECs were used in the *in-vitro* BBB model to investigate the trancytosis, uptake and toxicity of doxorubicin loaded quaternary ammonium β-cyclodextrin nanoparticles (142). The nanoparticle bound doxorubicin showed increased transcytosis across the BBB model compared to free doxorubicin (~2.49×10^6 cm/s compared with 1.1×10^6 cm/s) (142). The nanoparticles effectively shielded the doxorubicin,

preventing the efflux transporters from recognizing the substrate and thereby promoted delivery and efficient cell death of U87 human glioblastoma cells (142).

Further studies investigated the uptake of chitosan nanoparticles functionalised with a Fab fragment of amyloid-β antibody (IgG4.1) (145). The uptake of the targeted nanoparticles was compared with BSA coated chitosan nanoparticles as a control. The targeted chitosan nanoparticles showed increased uptake and transcytosis in the *in vitro* BBB model compared to the control nanoparticles (145). *In vivo*, uptake of fab targeted nanoparticles was also higher in the brain of the mice compared to the BSA control nanoparticles, especially in the cortex and hippocampus (141). However, the Fab targeted nanoparticles also showed greater clearance from plasma, likely due to the increased uptake in peripheral organs (kidney, liver, lung and spleen) (145).

More recently, a co-culture model of primary bovine BMECs and rat astrocytes were used to show enhanced transcytosis of gold nanoparticles conjugated to a THR-CLPFFD peptide (specific for the transferrin receptor) (143). The toxicity of the nanoparticles on the astrocytes and bovine BMECs was negligible with the targeted nanoparticles having an improved apparent permeability coefficient (Papp) compared to the untargeted (3.2 ± 0.04 10^{-7} cm/s and $9.7 \pm 0.3 \times 10^{-10}$ cm/s respectively) (143). Similarly the *in-vivo* data showed the THR-CLPFFD gold nanoparticles had the highest accumulation in rat brains compared to the untargeted and THR only gold nanoparticles (143). However, the overall amount of gold nanoparticles found in the brain was quite low (0.07% of the injected dose) (143).

Porcine

Primary porcine endothelial cells, cultured from pigs, yield robust models with high TEER (700 $\Omega.cm^2$) and low paracellular permeability ($1 \pm 0.4 \times 10^{-6}$ cm/s with sucrose in serum free media) (146). These endothelial cells can be harvested in large quantities as a starting material and the porcine *in-vitro* model possesses endothelial cell characteristics in terms of BBB specific proteins, transporters and enzymes (146–148). The porcine *in-vivo* models while not as numerous or well characterised as murine models, show more similarity to humans, in terms of size and brain structure (149, 150). A primary porcine BMEC BBB model was used to investigate the transport of oximes (an acetylcholinesterase reactivator) using human serum albumin nanoparticles, surface modified by PEGylation or by the addition of Apolipoprotein E. Both PEGylated and Apolipoprotein E modified human serum albumin nanoparticles were found to have low cellular toxicity, however, only Apolipoprotein E modified nanoparticles were able to transfer increased amounts of oximes across the BBB model (151).

The porcine BMEC model has also been used to investigate receptor-mediated uptake and transcytosis of PEG-coated Fe_3O_4 nanoparticles targeted to the brain with lactoferrin (152). Increased amounts of lactoferrin coated Fe_3O_4 nanoparticles were found to cross the BBB model in comparison to the untargeted (47% transport efficacy compared to 22.5%) (152). The presence of the PEG chains on the untargeted nanoparticle was thought to increase its uptake across the BBB model, though not as much to the same extent as the lactoferrin targeted NPs (152). *In-vivo* magnetic resonance imaging results in rats showed a greater exponential decrease in signal strength for the lactoferrin Fe_3O_4 nanoparticles 15 min after injection. This remained 24 h post-injection, particularly in the thalamus, brain stem and frontal cortex, but not the temporal cortex (152).

Human

The use of primary human endothelial cells in the creation of BBB models is less common in comparison to the BBB models from other species. This is most likely due to the ethical restraints associated with using human samples and the scarcity of brain tissue available to the researchers (132). However, a primary human BBB model would undoubtedly provide more clinically representative data regarding nanoparticle uptake, transcytosis and toxicity. Increased availability of primary human cells through commercial means (105) with easier and quicker isolation methods (132) may increase the use of primary human BBB models in research. Bonoiu *et al.* (2009) utilized primary human endothelial cells co-cultured with primary human astrocytes to investigate matrix metalloproteinase 9 (MMP-9) siRNA delivery using quantum dots. MMP-9-siRNA:quantum dot complexes reduced MMP-9 expression in the endothelial cells of the BBB model, resulting in a 30% increase in TEER (259 ± 10.61 Ω/cm^2 compared to 202 ± 14.14 Ω/cm^2) and a decrease in paracellular permeability after 48 h of transfection (105). More recent studies using primary human BBB models involved the investigation of the delivery of saquinivir (a protease inhibitor for treatment of HIV-1) and carmustine (a chemotherapeutic) to the CNS using solid lipid nanoparticles targeting the insulin receptor on human ECs (153, 154). These studies showed that the monoclonal antibody (MAb83-14) modified lipid nanoparticles could increase the uptake of both the drugs (saquinivir and carmustine) across the BBB model via the insulin receptor. Varying the composition of the nanoparticles also inhibited phagocytosis by RAW264.7 cells, which could potentially improve pharmacokinetics *in-vivo* (153, 154). However, these nanoparticles also exerted a negative impact on the BBB model TEER (~190 $\Omega.cm^2$ compared to 237 $\Omega.cm^2$ control) and permeability (~6.2×10^{-6} cm/s compared to 4.6×10^{-6} cm/s for control) (154). This was likely due to disorganization of the cytoskeletal structure of the endothelial cell monolayer (154).

Primary human *in vitro* models have also been used to investigate the uptake and transcytosis of gold nanoparticles functionalised with densely packed Bcl2L12 siRNA duplexes (155). The *in vitro* model consisted of primary human endothelial cells co-cultured with human astrocytes. 24 h after transfection the gold nanoparticles were found to have crossed the endothelial cell monolayer and uptake in the co-cultured astrocytes was observed by fluorescence microscopy (155). *In vivo*, the human glioma cell line U87 and tumour neurospheres derived from patients were grafted into mice to create a glioma mouse model. The siRNA gold nanoparticles were non-toxic in the glioma mouse model, nor in rats (155). The siRNA nanoparticles penetrated the BBB, achieved higher accumulation in the tumour tissue than normal brain tissue, resulting in significant reduction in both Bcl2L12 mRNA and protein in tumour tissue and increased survival rate in the treated glioma mouse model compared to the scrambled siRNA control (155).

Brain Endothelial Cells: Immortalised Cell Lines

There is a wide range of commercially available immortalised cell lines that have been used to investigate BBB function. These cells are usually isolated from mice, rats or humans. Immortalised cell lines have an advantage over primary cell models in that they can be sub-cultured and maintained for a number of passages, without compromising on their endothelial cell characteristics. This makes them useful for cellular binding, uptake and accumulation studies for nanoparticles. However, immortalised cell lines display very low TEER values and high paracellular permeability in comparison to primary cell models.

b.End3

The b.End3 cell line was created by immortalisation of brain endothelial cells procured from SV129 and Balb/c mice with the Polyoma middle T-antigen (156). It is the only commercial cell line available that is well characterised and shows expression of various transporters and receptors (157, 158). The use of the b.End3 cell line as a BBB model is limited to the cellular uptake, subcellular distribution, toxicity and receptor binding studies on the cell surface (159). In terms of paracellular permeability, bEnd3 cells are considered too "leaky" for screening drugs (157), but on the contrary, they have been used to investigate the transcytosis of macromolecules and nanoparticles (160).

The TEER values obtained using the b.End3 *in vitro* models have varied in the range of ~20–300 $\Omega.cm^2$ (49, 160, 161). The large variation in these values may be attributed to differences in experimental conditions i.e. cell monolayer alone and/or in co-culture with astrocytes and pericytes or with addition cAMP elevators or differences in length of time for which cells were cultured (49, 157, 160, 161).

In one report a bEnd.3 monolayer was used to assess the ability of transferrin coated magnetic silica PLGA nanoparticles to transport doxorubicin and paclitaxcel to the brain for glioma treatment (49). The drug loaded transferrin nanoparticles in the presence of a magnetic field showed the best trasncytosis through the BBB model (49). Levels of uptake and cytotoxicity in U87 MG human cells were also higher for the doxorubicin and paclitaxcel loaded transferrin nanoparticles compared to controls, with cytotoxicity similar to the free drug (49). This correlated well with an *in-vivo* glioma mouse model study, which showed a 47.5 fold reduction in tumour size for mice treated with the drug loaded magnetic transferrin nanoparticles compared to saline and non-targeted controls (49). The glioma bearing mice also exhibited no significant difference in weight compared to the saline control mice 20 days post injection indicating low toxicity *in vivo*.

hCMEC/D3

hCMEC/D3 cells are human endothelial cells isolated from an adult female and immortalized using hTERT and SV40 large T antigen transduction. This cell line has been very well characterised and displays many of the characteristics of endothelial cells including expression of claudins, occludin, enzymes and receptors (130). As a BBB model, the hCMEC/D3 cell line is characterized by decreased paracellular permeability and increased TEER values in comparison to other endothelial cell lines and is comparable to some of the primary cell line models (130). The hCMEC/D3 cell line has been used to investigate nanoparticle trancytosis by various research groups, establishing it as a well-validated model (162, 163). For example, transport of SiO_2 nanoparticles across the hCMEC/D3 BBB model has been reported (164). Through transcytosis studies and electron microscopy imaging, it was shown that, although the nanoparticles moved through the BBB model via the transcellular route, the filter used impeded the progress of the nanoparticles, despite the pore size being far larger than the nanoparticle diameter (0.4 μm pore PET filter with 50 nm nanoparticles) (164).

Another study utilised the hCMEC/D3 model to investigate the transcytosis of iron oxide nanoparticles functionalised with anti-pecam-1 antibody to target the BBB (165). The anti-pecam-1 nanoparticles showed increased affinity for hCMEC/D3 cells and increased transcytosis across the BBB model when compared to IgG functionalised control nanoparticles ($6.7 \pm 0.2 \times 10^{-6}$ compared to $4.8 \pm 0.2 \times 10^{-6}$ for IgG) (165). The biodistribution in mice of these nanoparticles showed significantly higher levels in the brain compared to the IgG control; however the majority distributed to the lungs, liver and spleen (165). Of the 0.11% of the injected dose that distributed to the brain, only 17 ± 12% of it reached the brain

parenchyma with the remaining 82 ± 12% associated with the endothelial cells (165). In the *in vitro* model it took 1 h for 4.5% of the anti-pecam-1 dose to be detected in the basolateral chamber, so a longer timepoint than 10 min may have been preferable for a proper investigation of the nanoparticle behaviour *in vivo* (165).

Other groups have used the hCMEC/D3 cell line to investigate transport of BBB targeted polymersomes (166, 167), immunoliposomes (162) and solid lipid nanoparticles functionalized for targeted brain delivery (168).

Pluripotent Stem Cells

More recently, researchers have developed human endothelial cells from an induced pluripotent stem cell line IMR90-4 (169). The resultant human endothelial cells were found to generate a very high TEER value (1,450 ± 150 $\Omega.cm^2$), low paracellular permeability (3.4×10^{-5} cm/min) and expressed many transcripts for receptors and transporters which were characteristic of BMECs (169). These paracellular permeability and TEER values were found to be superior to the commonly used primary and immortalized cell models (169). Although this model is a closer representation of the *in vivo* environment, it can be more complex to set up and requires further characterization as an *in-vitro* model. Additional work by this group resulted in an all human BBB model using stem-cell derived components as well as primary human cells (170). This model achieved a TEER of over 5,000 $\Omega.cm^2$, with the addition of retinoic acid (170).

In comparison to the above mentioned b.End3 cells the hCMEC/D3 cell line is considered more useful as it is more fully characterized and is a human-derived cell line. Further research on and development of the process of stem cell differentiation and the increased availability of stem cell lines will surely lead to greater use of these models in nanoparticle research. There also exists an option to create BBB models using induced pluripotent stem cells from diseased patients. This would allow for the testing of nanoformulations on human *in-vitro* models which are more accurate representations of the neurodegenerative disorder.

MDCK and Caco 2

Madin-Darby Canine kidney (MDCK) cells and the human colorectal adenocarcinoma (Caco-2) cells are widely used immortalised epithelial cell lines. They have shown to produce a tight monolayer after culturing in suitable conditions for 3–4 days for MDCK cells and 3 weeks for Caco 2 cells. However, the main disadvantage of these cells in application to BBB model is their non-cerebral origin. Their cell architecture is very different from brain endothelial cells with narrow, tall cells compared to long spindle shape of neuronal cells. In addition, they possess microvilli on their apical surface (125, 171). However, these cells have extensively been used to investigate the transcytosis of nanoparticles. Zhao *et al.* (2012b) used a variety of imaging techniques to investigate the transcytosis and cellular localisation of polymeric micelles containing fluorescent Coumarin 6 probes in a MDCK *in vitro* model. The uptake mechanism was determined to be mostly by a clathrin mediated pathway along with another mechanism, which was independent of clathrin and calveolae (172). Kirby *et al.*(2013) used a Caco-2 *in-vitro* model to investigate the uptake of PEG-PLGA-loperamide nanoparticles. Uptake studies showed that increasing amounts of PEG (5, 10 and 15%) produce improved uptake in the caco-2 BBB model (173). *In-vivo*, the intranasally administered PEG-PLGA nanoparticles enhanced the delivery of loperamide to the brain as indicated by analgesic effect in mice compared to non-PEGylated PLGA nanoparticles and free loperamide (173). Though the 15% PEG-PLGA gave the highest uptake *in vitro*, the most effective formulation *in vivo* was the 10% PEG-PLGA which achieved a higher and sustained antinociceptive effect (173).

Novel Models

The presence of shear stress due to the simulated blood flow has been shown to improve BBB characteristics, such as, the expression of tight-junction proteins (174) and certain *in-vitro* BBB models have been developed that incorporate this. These include the dynamic *in-vitro* BBB model (DIV BBB) (174) and the microfluidics BBB model on chip (μBBB) (175). Both of these models display higher TEER values and reduced paracellular permeability in comparison to the static transwell culture models. The DIV-BBB model consists of endothelial cells cultured on the inner side (luminal surface) of hollow tubes, pre-coated with fibronectin, and astrocytes cultured on the outer side of the tubes (abluminal surface), pre-coated with poly-l-lysine. This leads to more realistic cell architecture, with a TEER of 524 ± 26.7 $\Omega.cm^2$ (174). The μBBB model consists of a co-culture of brain endothelial cells on the upper side of a porous membrane and astrocytes on the lower side. In addition to the dynamic flow across the BMECs, the μBBB model allows for the observation of the cell morphology while being grown on the membrane. This is not possible with the DIV model, due to the thickness of the hollow tubes used to culture the cells. The TEER value reported for the μBBB model was >250 $\Omega.cm^2$ (175). In terms of cost, although the μBBB model requires less materials, it is not as representative of the neurovascular unit as the DIV BBB model. For these reasons, the μBBB model is considered more suitable for high throughput screening of nano-drug/solute formulations (128, 175).

In summary, a wide range of BBB models, with inherent advantages and disadvantages, have been used to study the CNS delivery potential of NPs. In specific cases the *in vitro* models have successfully identified NP formulations which

subsequently demonstrated *in vivo* efficacy (Table III). This gives encouragement to the utility of such *in vitro* systems. However, the translatability from animal models to human therapeutics still needs validation. Moreover, it is also worth pointing out that a major limitation of *in vitro* models is the inability to predict the extent of *in vivo* delivery to the brain *versus* biodistribution to other organs. With increasing global pressure to reduce the number of animal experiments (176) there is a need to investigate and design more physiologically relevant *in vitro* BBB models capable of more accurately predicting *in vivo* performance of NPs.

Conclusion and Perspectives

Delivery of therapeutics across the BBB represents a major rate limiting step to the treatment of brain disorders. The barrier function of the BBB, combined with scarcity of

Table III Comparison of *In vitro Versus In vivo* Results for Different BBB Models and Nanoformulations

In vitro model	Nanoformulation	Cargo	*In vivo* model	Prediction of *In vivo* performance	Reference
Primary rat BMEC and astrocytes	Triton X-100 and Lutensol	Kynurenic acid (Product of L-tryptophan metabolism)	Wistar rat	*In vitro*: increased transcytosis with surfactant-based nanoformulations. *In vivo*: increased response in the hippocampus as indicated by electrophysiology.	(138)
Primary rat BMEC and C6 glioma cells	Tamoxifen-Tf functionalised liposomes	Epirubicin	C6 glioma rat model (C6 cells grafted into Wistar rat brain)	*In vitro*: highest transport and cytotoxicity with the targeted NPs. *In vivo*: significant inhibition of tumour growth following treatment with targeted NPs.	(139)
Primary mouse BMEC	RVG-PAMAM dendrimer	Luciferase DNA	Nude mouse and BALB/c mouse	*In vitro*: increased transcytosis and higher uptake with RVG targeted NPs *In vivo*: Higher levels of luciferase activity in the brain with targeted NP compared to untargeted control.	(140)
Primary Bovine BMEC	amyloid-β antibody fragment chitosan	FITC-BSA (*in vitro* only)	B6/SJL mouse	*In vitro*: increased transcytosis with targeted *vs* untargeted NP *In vivo*: enhanced brain uptake with targeted NPs	(145)
Primary Bovine BMEC	THR-CLPFFD (peptide) gold NPs	None	Sprague Dawley rat	*In vitro*: transcytosis was achieved *In vivo*: low levels of NPs in the brain	(143)
Primary Porcine BMEC	Lactoferrin coated Fe_3O_4 -NPs	None	Sprague Dawley rat	*In vitro*: higher transcytosis with Lactoferrin coated Fe_3O_4 *vs* PEGylated control. *In vivo*: Targeted showed highest uptake compared to control	(152)
Primary human BMEC and astrocytes	siRNA functionalised gold NPs	Bcl2L12 siRNA	Sprague Dawley rat and glioma mouse model (U87 cells or patient derived tumour neurospheres grafted into CB17 SCID mouse brain)	*In vitro*: trancytosis across the BBB model and uptake in U87 cell and human tumour neurospheres. *In vivo*: Significant mRNA and protein knockdown with little toxicity in either rat or glioma bearing mice.	(155)
b.End3 immortalized BMEC	Tf coated magnetic silica PLGA NPs	Doxorubicin and Paclitaxel	Glioma mouse model (U87 glioma cells grafted into BALB/c nude mouse brain)	*In vitro*: highest transcytosis with Tf NPs *In vivo*: greatest inhibition of tumour growth with Tf doxorubicin paclitaxel NPs *vs* untargeted or Tf targeted doxorubicin and paclitaxel NPs alone.	(49)
hCMEC/D3 immortalized BMEC	Anti-pecam-1 functionalised Fe_3O_4 NPs	None	Sprague Dawley rat	*In vitro*: greater trancytosis with targeted NPs *vs* untargeted *In vivo*: achieved brain uptake at limited levels	(165)
Caco-2 immortalized EC	PEG-PLGA NPs	Loperamide	C57BL6 mouse	*In vitro*: The highest uptake with 15% PEG-PLGA-loperamide NPs *In vivo*: in contrast the 10% PEG-PLGA-loperamide NPs were more effective	(173)

BMEC Brain Microvascular Endothelial Cells, *NPs* nanoparticles, *BBB* blood-brain barrier, *EC* endothelial cells, *PLGA* Poly(lactic-co-glycolic acid), *BSA* Bovine Serum Albumin, *PEG* Polyethylene glycol, *PAMAM* Polyamidoamine, *RVG* Rabies virus glycoprotein, *PLGA* Poly(lactic-co-glycolic acid)

information about some CNS disorders, has led to prolonged development periods and increased failure rates of CNS therapeutics in clinical trials (177). However, nanoformulations have shown promising preclinical success in delivering therapeutics which are otherwise inherently impermeable to the BBB. A wide variety of nanoformulations incorporating a range of different materials both biodegradable and non-biodegradable have been evaluated. The design of individual formulations tends to be complex- in addition to the core material e.g. a polymer, other functional excipients including PEG and targeting ligands are engineered into the particle. While certain formulations have produced exciting and promising results *in vitro*, and in some cases *in-vivo*, few have entered clinical trial and no product is to date clinically available.

To advance this technology to the clinic issues of stability and reproducibility during formulation, production, and scale-up need to be addressed. Most of the development and synthetic procedures of nanoparticles involve a multistep protocol incorporating several individual components (178). Each step requires optimisation prior to scale up. The limiting factors that preserve the consistency of nanoparticles, in terms of its physiochemical and biological activity, need to be identified. For example, the stability of nanoparticles against aggregation is a major challenge, which can significantly impact the shelf-life and half-life of the nanoparticles in the body. Thus, extensive experimentation in terms of size distribution and composition is essential to identify and optimise a robust design and a reproducible product yet (178). Other important factors to consider are the critical manufacturing/process parameters such as sheer force, temperature, pH conditions, storage and sterilization techniques, which may influence the stability and purity of the product (178). In addition, due to the bioactive nature of these nanoformulations, further investigation is needed to understand the formulation-based cellular uptake mechanisms and target specificity used to minimise unintended distribution to other non-specific cells and organs in the body following administration (179, 180). These issues are likely to be regulatory requirements for nanomedicines, which are not routinely encountered with conventional medicines. In general, while research on the topic of nano-toxicity is ongoing, results and conclusions are often conflicting and the availability of more informative methods specifically designed for toxicity testing of such formulations may help to alleviate this issue.

An additional barrier to the advancement of nanomedicines in the treatment of CNS disorders is the lack of suitably validated *in-vitro* models capable of accurately assessing delivery potential and predicting *in vivo* performance. This review addresses the ability of currently used *in vitro* BBB models to predict *in vivo* performance. Despite advances in the development of various *in-vitro* BBB models, many have significant limitations and no ideal model has been identified. The choice of the model is critical and may often be dictated by the aims of the particular study; simple cost-effective models may suffice for high throughput screening while more complex co-culture models may be necessary for evaluating the delivery potential of elaborate formulations. Recent innovative models including the dynamic *in-vitro* BBB model (DIV BBB) (128) and the microfluidics BBB model on chip (μBBB) (175) which simulate more closely the physical aspects of the BBB offer an improved representation of the *in-vivo* conditions.

In summary, while exciting and innovative nanoformulations are becoming increasingly available, discovery and development in the area of *in-vitro* BBB models has not advanced at the same pace. In order to accurately evaluate the therapeutic significance of such formulations for treatment of CNS disorders and accelerate advancement to the clinic more physiologically relevant *in-vitro* models of the BBB are urgently needed.

REFERENCES

1. National Institute of Neurological Disorders and Stroke. National Institute of Neurological Disorders and Stroke. National Institute of Neurological Disorders and Stroke 2014 02-07-14. Available from: http://www.ninds.nih.gov/about_ninds/ninds_overview.htm.
2. World Health Organization. *Dementia: A public health priority*. In.: World Health Organization; 2012.
3. Kowal SL, Dall TM, Chakrabarti R, Storm MV, Jain A. The current and projected economic burden of Parkinson's disease in the United States. Mov Disord. 2013;28(3):311–8.
4. Olesen J, Gustavsson A, Svensson M, Wittchen HU, Jonsson B, group Cs, et al. The economic cost of brain disorders in Europe. Eur J Neurol. 2012;19(1):155–62.
5. Thies W, Bleiler L, Alzheimer's A. 2013 Alzheimer's disease facts and figures. Alzheimers Dement. 2013;9(2):208–45.
6. Thakker DR, Natt F, Husken D, van der Putten H, Maier R, Hoyer D, et al. siRNA-mediated knockdown of the serotonin transporter in the adult mouse brain. Mol Psychiatry. 2005;10(8):782–9. 714.
7. Liu Y, Li J, Shao K, Huang R, Ye L, Lou J, et al. A leptin derived 30-amino-acid peptide modified pegylated poly-L-lysine dendrigraft for brain targeted gene delivery. Biomaterials. 2010;31(19):5246–57.
8. Lindqvist A, Rip J, Gaillard PJ, Bjorkman S, Hammarlund-Udenaes M. Enhanced brain delivery of the opioid peptide DAMGO in glutathione pegylated liposomes: a microdialysis study. Mol Pharm. 2013;10(5):1533–41.
9. Li Y, He H, Jia X, Lu WL, Lou J, Wei Y. A dual-targeting nanocarrier based on poly(amidoamine) dendrimers conjugated with transferrin and tamoxifen for treating brain gliomas. Biomaterials. 2012;33(15):3899–908.
10. de Boer AG, Gaillard PJ. Drug targeting to the brain. Annu Rev Pharmacol Toxicol. 2007;47:323–55.
11. Abbott NJ, Ronnback L, Hansson E. Astrocyte-endothelial interactions at the blood-brain barrier. Nat Rev Neurosci. 2006;7(1):41–53.
12. Sa-Pereira I, Brites D, Brito MA. Neurovascular unit: a focus on pericytes. Mol Neurobiol. 2012;45(2):327–47.
13. Abbott NJ. Astrocyte-endothelial interactions and blood-brain barrier permeability. J Anat. 2002;200(6):629–38.
14. Ballabh P, Braun A, Nedergaard M. The blood-brain barrier: an overview: structure, regulation, and clinical implications. Neurobiol Dis. 2004;16(1):1–13.

15. Cristante E, McArthur S, Mauro C, Maggioli E, Romero IA, Wylezinska-Arridge M, et al. Identification of an essential endogenous regulator of blood-brain barrier integrity, and its pathological and therapeutic implications. Proc Natl Acad Sci U S A. 2013;110(3):832–41.
16. Wolburg H, Lippoldt A. Tight junctions of the blood-brain barrier: development, composition and regulation. Vasc Pharmacol. 2002;38(6):323–37.
17. Banks WA. Characteristics of compounds that cross the blood-brain barrier. BMC Neurol. 2009;9 Suppl 1:S3.
18. Mikitsh JL, Chacko AM. Pathways for small molecule delivery to the central nervous system across the blood-brain barrier. Perspect Med Chem. 2014;6:11–24.
19. Pardridge WM. Drug transport across the blood-brain barrier. J Cereb Blood Flow Metab. 2012;32(11):1959–72.
20. Begley DJ. Delivery of therapeutic agents to the central nervous system: the problems and the possibilities. Pharmacol Ther. 2004;104(1):29–45.
21. Pardridge WM. Drug and gene targeting to the brain with molecular Trojan horses. Nat Rev Drug Discov. 2002;1(2):131–9.
22. Domínguez A, Álvarez A, Hilario E, Suarez-Merino B, Goñi-de-Cerio F. Central nervous system diseases and the role of the blood-brain barrier in their treatment. Neurosci Discov. 2013;1(1).
23. Simionescu M, Gafencu A, Antohe F. Transcytosis of plasma macromolecules in endothelial cells: a cell biological survey. Microsc Res Tech. 2002;57(5):269–88.
24. Abbott NJ, Patabendige AA, Dolman DE, Yusof SR, Begley DJ. Structure and function of the blood-brain barrier. Neurobiol Dis. 2010;37(1):13–25.
25. Smith MW, Gumbleton M. Endocytosis at the blood-brain barrier: from basic understanding to drug delivery strategies. J Drug Target. 2006;14(4):191–214.
26. Perez-Martinez FC, Guerra J, Posadas I, Cena V. Barriers to non-viral vector-mediated gene delivery in the nervous system. Pharm Res. 2011;28(8):1843–58.
27. Dauchy S, Dutheil F, Weaver RJ, Chassoux F, Daumas-Duport C, Couraud PO, et al. ABC transporters, cytochromes P450 and their main transcription factors: expression at the human blood-brain barrier. J Neurochem. 2008;107(6):1518–28.
28. O'Brien FE, Dinan TG, Griffin BT, Cryan JF. Interactions between antidepressants and P-glycoprotein at the blood-brain barrier: clinical significance of *in vitro* and *in vivo* findings. Br J Pharmacol. 2012;165(2):289–312.
29. Ohtsuki S, Terasaki T. Contribution of carrier-mediated transport systems to the blood-brain barrier as a supporting and protecting interface for the brain; importance for CNS drug discovery and development. Pharm Res. 2007;24(9):1745–58.
30. Forster C. Tight junctions and the modulation of barrier function in disease. Histochem Cell Biol. 2008;130(1):55–70.
31. Persidsky Y, Ramirez SH, Haorah J, Kanmogne GD. Blood-brain barrier: structural components and function under physiologic and pathologic conditions. J Neuroimmune Pharm. 2006;1(3):223–36.
32. De Rosa G, Salzano G, Caraglia M, Abbruzzese A. Nanotechnologies: a strategy to overcome blood-brain barrier. Curr Drug Metab. 2012;13(1):61–9.
33. Kesharwani P, Gajbhiye V, Jain NK. A review of nanocarriers for the delivery of small interfering RNA. Biomaterials. 2012;33(29):7138–50.
34. O'Mahony AM, Godinho BM, Cryan JF, O'Driscoll CM. Non-viral nanosystems for gene and small interfering RNA delivery to the central nervous system: formulating the solution. J Pharm Sci. 2013;102(10):3469–84.
35. Kreuter J. Nanoparticulate systems in drug delivery and targeting. J Drug Target. 1995;3(3):171–3.
36. LaVan DA, McGuire T, Langer R. Small-scale systems for *in vivo* drug delivery. Nat Biotechnol. 2003;21(10):1184–91.
37. Barbu E, Molnar E, Tsibouklis J, Gorecki DC. The potential for nanoparticle-based drug delivery to the brain: overcoming the blood-brain barrier. Expert Opin Drug Deliv. 2009;6(6):553–65.
38. Hillaireau H, Couvreur P. Nanocarriers' entry into the cell: relevance to drug delivery. Cell Mol Life Sci. 2009;66(17):2873–96.
39. Hillyer JF, Albrecht RM. Gastrointestinal persorption and tissue distribution of differently sized colloidal gold nanoparticles. J Pharm Sci. 2001;90(12):1927–36.
40. Sarin H, Kanevsky AS, Wu H, Brimacombe KR, Fung SH, Sousa AA, et al. Effective transvascular delivery of nanoparticles across the blood-brain tumor barrier into malignant glioma cells. J Transl Med. 2008;6:80.
41. Malhotra M, Tomaro-Duchesneau C, Saha S, Prakash S. Intranasal, siRNA delivery to the brain by TAT/MGF tagged PEGylated chitosan nanoparticles. J Pharm. 2013;2013:10.
42. Oberdorster G, Sharp Z, Atudorei V, Elder A, Gelein R, Kreyling W, et al. Translocation of inhaled ultrafine particles to the brain. Inhal Toxicol. 2004;16(6–7):437–45.
43. Dhuria SV, Hanson LR, Frey 2nd WH. Intranasal delivery to the central nervous system: mechanisms and experimental considerations. J Pharm Sci. 2010;99(4):1654–73.
44. Yao L, Song Q, Bai W, Zhang J, Miao D, Jiang M, et al. Facilitated brain delivery of poly (ethylene glycol)-poly (lactic acid) nanoparticles by microbubble-enhanced unfocused ultrasound. Biomaterials. 2014;35(10):3384–95.
45. Wohlfart S, Gelperina S, Kreuter J. Transport of drugs across the blood-brain barrier by nanoparticles. J Control Release. 2012;161(2):264–73.
46. Mahon E, Salvati A, Baldelli Bombelli F, Lynch I, Dawson KA. Designing the nanoparticle-biomolecule interface for "targeting and therapeutic delivery". J Control Release. 2012;161(2):164–74.
47. Masserini M. Nanoparticles for brain drug delivery. ISRN Biochem. 2013;2013:18.
48. Kumar P, Wu H, McBride JL, Jung KE, Kim MH, Davidson BL, et al. Transvascular delivery of small interfering RNA to the central nervous system. Nature. 2007;448(7149):39–43.
49. Cui Y, Xu Q, Chow PK, Wang D, Wang CH. Transferrin-conjugated magnetic silica PLGA nanoparticles loaded with doxorubicin and paclitaxel for brain glioma treatment. Biomaterials. 2013;34(33):8511–20.
50. Shilo M, Motiei M, Hana P, Popovtzer R. Transport of nanoparticles through the blood-brain barrier for imaging and therapeutic applications. Nanoscale. 2014;6(4):2146–52.
51. Beduneau A, Saulnier P, Benoit JP. Active targeting of brain tumors using nanocarriers. Biomaterials. 2007;28(33):4947–67.
52. Aktas Y, Yemisci M, Andrieux K, Gursoy RN, Alonso MJ, Fernandez-Megia E, et al. Development and brain delivery of chitosan-PEG nanoparticles functionalized with the monoclonal antibody OX26. Bioconjug Chem. 2005;16(6):1503–11.
53. Pardridge WM. Brain drug targeting and gene technologies. Jpn J Pharmacol. 2001;87(2):97–103.
54. Pardridge WM. Preparation of Trojan horse liposomes (THLs) for gene transfer across the blood-brain barrier. Cold Spring Harb Protoc. 2010;2010(4):pdb prot5407.
55. Arruebo M, Valladares M, #243, nica, Gonz, #225, lez-Fern, #225, ndez, #193, frica. Antibody-conjugated nanoparticles for biomedical applications. J Nanomater. 2009;2009.
56. Soni V, Kohli DV, Jain SK. Transferrin-conjugated liposomal system for improved delivery of 5-fluorouracil to brain. J Drug Target. 2008;16(1):73–8.
57. Gaillard PJ, Appeldoorn CC, Rip J, Dorland R, van der Pol SM, Kooij G, et al. Enhanced brain delivery of liposomal methylprednisolone improved therapeutic efficacy in a model of neuroinflammation. J Control Release. 2012;164(3):364–9.
58. Orthmann A, Zeisig R, Suss R, Lorenz D, Lemm M, Fichtner I. Treatment of experimental brain metastasis with MTO-liposomes:

impact of fluidity and LRP-targeting on the therapeutic result. Pharm Res. 2012;29(7):1949–59.
59. Artzner F, Zantl R, Radler JO. Lipid-DNA and lipid-polyelectrolyte mesophases: structure and exchange kinetics. Cell Mol Biol (Noisy-le-grand). 2000;46(5):967–78.
60. Mochizuki S, Kanegae N, Nishina K, Kamikawa Y, Koiwai K, Masunaga H, et al. The role of the helper lipid dioleoylphosphatidylethanolamine (DOPE) for DNA transfection cooperating with a cationic lipid bearing ethylenediamine. Biochim Biophys Acta. 2013;1828(2):412–8.
61. Chen H, Tang L, Qin Y, Yin Y, Tang J, Tang W, et al. Lactoferrin-modified procationic liposomes as a novel drug carrier for brain delivery. Eur J Pharm Sci. 2010;40(2):94–102.
62. Zhao M, Chang J, Fu X, Liang C, Liang S, Yan R, et al. Nano-sized cationic polymeric magnetic liposomes significantly improves drug delivery to the brain in rats. J Drug Target. 2012;20(5):416–21.
63. Kaur IP, Bhandari R, Bhandari S, Kakkar V. Potential of solid lipid nanoparticles in brain targeting. J Control Release. 2008;127(2):97–109.
64. Blasi P, Giovagnoli S, Schoubben A, Ricci M, Rossi C. Solid lipid nanoparticles for targeted brain drug delivery. Adv Drug Deliv Rev. 2007;59(6):454–77.
65. Martins S, Tho I, Reimold I, Fricker G, Souto E, Ferreira D, et al. Brain delivery of camptothecin by means of solid lipid nanoparticles: formulation design, *in vitro* and *in vivo* studies. Int J Pharm. 2012;439(1–2):49–62.
66. Goppert TM, Muller RH. Polysorbate-stabilized solid lipid nanoparticles as colloidal carriers for intravenous targeting of drugs to the brain: comparison of plasma protein adsorption patterns. J Drug Target. 2005;13(3):179–87.
67. University of California. A Phase I trial of Nanoliposomal CPT-11 (NL CPT-11) in Patients with recurrent high-grade Gliomas. Available from: http://clinicaltrials.gov/show/NCT00734682.
68. University Hospital B. Phase II study evaluating the combination pegylated liposomal doxorubicin and dexamethasone for the treatment of immunocompetent patients with cerebral lymphoma relapsed or refractory to first-line chemotherapy containing high dose methotrexate (MTXHD) and / or high-dose Cytarabine. Available from: http://clinicaltrials.gov/ct2/show/NCT01848652.
69. The University of Texas Health Science Center at San Antonio. A dual Phase 1/2, Investigator initiated study to determine the maximum tolerated dose, safety, and efficacy of rhenium nanoliposomes in recurrent Glioblastoma. Available from: http://clinicaltrials.gov/ct2/show/NCT01906385.
70. Kabanov AV, Batrakova EV, Melik-Nubarov NS, Fedoseev NA, Dorodnich TY, Alakhov VY, et al. A new class of drug carriers: micelles of poly(oxyethylene)-poly(oxypropylene) block copolymers as microcontainers for drug targeting from blood in brain. J Control Release. 1992;22(2):141–57.
71. Batrakova EV, Miller DW, Li S, Alakhov VY, Kabanov AV, Elmquist WF. Pluronic P85 enhances the delivery of digoxin to the brain: *in vitro* and *in vivo* studies. J Pharmacol Exp Ther. 2001;296(2):551–7.
72. Kim JY, Choi WI, Kim YH, Tae G. Brain-targeted delivery of protein using chitosan- and RVG peptide-conjugated, pluronic-based nano-carrier. Biomaterials. 2013;34(4):1170–8.
73. Ricci M, Blasi P, Giovagnoli S, Rossi C. Delivering drugs to the central nervous system: a medicinal chemistry or a pharmaceutical technology issue? Curr Med Chem. 2006;13(15):1757–75.
74. Kreuter J. Influence of the surface properties on nanoparticle-mediated transport of drugs to the brain. J Nanosci Nanotechnol. 2004;4(5):484–8.
75. Gao K, Jiang X. Influence of particle size on transport of methotrexate across blood brain barrier by polysorbate 80-coated polybutylcyanoacrylate nanoparticles. Int J Pharm. 2006;310(1–2):213–9.
76. Alyautdin R, Gothier D, Petrov V, Kharkevich D, Kreuter J. Analgesic activity of the hexapeptide dalargin adsorbed on the surface of polysorbate 80-coated poly (butyl cyanoacrylate) nanoparticles. Eur J Pharm Biopharm. 1995;41(1):44–8.
77. Tian X-H, Lin X-N, Wei F, Feng W, Huang Z-C, Wang P, et al. Enhanced brain targeting of temozolomide in polysorbate-80 coated polybutylcyanoacrylate nanoparticles. Int J Nanomedicine. 2011;6:445–52.
78. Schneider T, Becker A, Ringe K, Reinhold A, Firsching R, Sabel BA. Brain tumor therapy by combined vaccination and antisense oligonucleotide delivery with nanoparticles. J Neuroimmunol. 2008;195(1–2):21–7.
79. Kim D-H, Martin DC. Sustained release of dexamethasone from hydrophilic matrices using PLGA nanoparticles for neural drug delivery. Biomaterials. 2006;27(15):3031–7.
80. Gao X, Wu B, Zhang Q, Chen J, Zhu J, Zhang W, et al. Brain delivery of vasoactive intestinal peptide enhanced with the nanoparticles conjugated with wheat germ agglutinin following intranasal administration. J Control Release. 2007;121(3):156–67.
81. Choonara YE, Pillay V, Ndesendo VM, du Toit LC, Kumar P, Khan RA, et al. Polymeric emulsion and crosslink-mediated synthesis of super-stable nanoparticles as sustained-release anti-tuberculosis drug carriers. Colloids Surf B: Biointerfaces. 2011;87(2):243–54.
82. Kumar M, Pandey RS, Patra KC, Jain SK, Soni ML, Dangi JS, et al. Evaluation of neuropeptide loaded trimethyl chitosan nanoparticles for nose to brain delivery. Int J Biol Macromol. 2013;61:189–95.
83. Md S, Khan RA, Mustafa G, Chuttani K, Baboota S, Sahni JK, et al. Bromocriptine loaded chitosan nanoparticles intended for direct nose to brain delivery: pharmacodynamic, pharmacokinetic and scintigraphy study in mice model. Eur J Pharm Sci. 2013;48(3):393–405.
84. Maiti PK, Çağın T, Wang G, Goddard WA. Structure of PAMAM dendrimers: generations 1 through 11. Macromolecules. 2004;37(16):6236–54.
85. Albertazzi L, Gherardini L, Brondi M, Sulis Sato S, Bifone A, Pizzorusso T, et al. *In vivo* distribution and toxicity of PAMAM dendrimers in the central nervous system depend on their surface chemistry. Mol Pharm. 2013;10(1):249–60.
86. Kannan S, Dai H, Navath RS, Balakrishnan B, Jyoti A, Janisse J, et al. Dendrimer-based postnatal therapy for neuroinflammation and cerebral palsy in a rabbit model. Sci Transl Med. 2012;4(130):130ra146.
87. Ye Y, Sun Y, Zhao H, Lan M, Gao F, Song C, et al. A novel lactoferrin-modified beta-cyclodextrin nanocarrier for brain-targeting drug delivery. Int J Pharm. 2013;458(1):110–7.
88. Gil ES, Wu L, Xu L, Lowe TL. Beta-cyclodextrin-poly(beta-amino ester) nanoparticles for sustained drug delivery across the blood-brain barrier. Biomacromolecules. 2012;13(11):3533–41.
89. O'Mahony AM, O'Neill MJ, Godinho BM, Cryan JF, O'Driscoll CM. Cyclodextrins for Non-viral gene and siRNA delivery. Pharm Nanotechnol. 2012;1(1):6–14.
90. O'Mahony AM, Godinho BM, Ogier J, Devocelle M, Darcy R, Cryan JF, et al. Click-modified cyclodextrins as nonviral vectors for neuronal siRNA delivery. ACS Chem Neurosci. 2012;3(10):744–52.
91. O'Mahony AM, Desgranges S, Ogier J, Quinlan A, Devocelle M, Darcy R, et al. *In vitro* investigations of the efficacy of cyclodextrin-siRNA complexes modified with lipid-PEG-Octaarginine: towards a formulation strategy for non-viral neuronal siRNA delivery. Pharm Res. 2013;30(4):1086–98.
92. O'Mahony AM, Ogier J, Darcy R, Cryan JF, O'Driscoll CM. Cationic and PEGylated amphiphilic cyclodextrins: co-formulation opportunities for neuronal sirna delivery. PLoS ONE. 2013;8(6):e66413.
93. O'Mahony AM, Doyle D, Darcy R, Cryan JF, O'Driscoll CM. Characterisation of cationic amphiphilic cyclodextrins for neuronal

delivery of siRNA: effect of reversing primary and secondary face modifications. Eur J Pharm Sci. 2012;47(5):896–903.
94. Godinho BM, Ogier JR, Darcy R, O'Driscoll CM, Cryan JF. Self-assembling modified β-cyclodextrin nanoparticles as neuronal siRNA delivery vectors: focus on Huntington's disease. Mol Pharm. 2013;10(2):640–9.
95. Godinho BM, McCarthy DJ, Torres-Fuentes C, Beltran CJ, McCarthy J, Quinlan A, et al. Differential nanotoxicological and neuroinflammatory liabilities of non-viral vectors for RNA interference in the central nervous system. Biomaterials. 2014;35(1):489–99.
96. Levy R, Shaheen U, Cesbron Y, See V. Gold nanoparticles delivery in mammalian live cells: a critical review. Nano Rev. 2010;1.
97. Sonavane G, Tomoda K, Makino K. Biodistribution of colloidal gold nanoparticles after intravenous administration: effect of particle size. Colloids Surf B: Biointerfaces. 2008;66(2):274–80.
98. Bonoiu AC, Bergey EJ, Ding H, Hu R, Kumar R, Yong KT, et al. Gold nanorod—siRNA induces efficient *in vivo* gene silencing in the rat hippocampus. Nanomed (Lond). 2011;6(4):617–30.
99. Schleh C, Semmler-Behnke M, Lipka J, Wenk A, Hirn S, Schaffler M, et al. Size and surface charge of gold nanoparticles determine absorption across intestinal barriers and accumulation in secondary target organs after oral administration. Nanotoxicology. 2012;6(1):36–46.
100. Roy I, Stachowiak MK, Bergey EJ. Nonviral gene transfection nanoparticles: function and applications in the brain. Nanomed: Nanotechnol, Biol Med. 2008;4(2):89–97.
101. Memorial Sloan-Kettering Cancer Center. PET imaging of patients with melanoma and malignant brain tumors using an 124I-labeled cRGDY silica nanomolecular particle tracer: A microdosing study. Available from: http://clinicaltrials.gov/ct2/show/NCT01266096.
102. Benezra M, Penate-Medina O, Zanzonico PB, Schaer D, Ow H, Burns A, et al. Multimodal silica nanoparticles are effective cancer-targeted probes in a model of human melanoma. J Clin Invest. 2011;121(7):2768–80.
103. Baoukina S, Monticelli L, Risselada HJ, Marrink SJ, Tieleman DP. The molecular mechanism of lipid monolayer collapse. Proc Natl Acad Sci U S A. 2008;105(31):10803–8.
104. Xu G, Mahajan S, Roy I, Yong KT. Theranostic quantum dots for crossing blood-brain barrier and providing therapy of HIV-associated encephalopathy. Front Pharmacol. 2013;4:140.
105. Bonoiu A, Mahajan SD, Ye L, Kumar R, Ding H, Yong KT, et al. MMP-9 gene silencing by a quantum dot-siRNA nanoplex delivery to maintain the integrity of the blood brain barrier. Brain Res. 2009;1282:142–55.
106. Chan WC, Maxwell DJ, Gao X, Bailey RE, Han M, Nie S. Luminescent quantum dots for multiplexed biological detection and imaging. Curr Opin Biotechnol. 2002;13(1):40–6.
107. Xu G, Yong KT, Roy I, Mahajan SD, Ding H, Schwartz SA, et al. Bioconjugated quantum rods as targeted probes for efficient transmigration across an *in vitro* blood-brain barrier. Bioconjug Chem. 2008;19(6):1179–85.
108. Brooks H, Lebleu B, Vives E. Tat peptide-mediated cellular delivery: back to basics. Adv Drug Deliv Rev. 2005;57(4):559–77.
109. Choi CH, Alabi CA, Webster P, Davis ME. Mechanism of active targeting in solid tumors with transferrin-containing gold nanoparticles. Proc Natl Acad Sci U S A. 2010;107(3):1235–40.
110. Nakase I, Tadokoro A, Kawabata N, Takeuchi T, Katoh H, Hiramoto K, et al. Interaction of arginine-rich peptides with membrane-associated proteoglycans is crucial for induction of actin organization and macropinocytosis. Biochemistry. 2007;46(2):492–501.
111. Vives E, Richard JP, Rispal C, Lebleu B. TAT peptide internalization: seeking the mechanism of entry. Curr Protein Pept Sci. 2003;4(2):125–32.
112. Muratovska A, Eccles MR. Conjugate for efficient delivery of short interfering RNA (siRNA) into mammalian cells. FEBS Lett. 2004;558(1–3):63–8.
113. Simeoni F, Morris MC, Heitz F, Divita G. Insight into the mechanism of the peptide-based gene delivery system MPG: implications for delivery of siRNA into mammalian cells. Nucleic Acids Res. 2003;31(11):2717–24.
114. Kim WJ, Christensen LV, Jo S, Yockman JW, Jeong JH, Kim YH, et al. Cholesteryl oligoarginine delivering vascular endothelial growth factor siRNA effectively inhibits tumor growth in colon adenocarcinoma. Mol Ther. 2006;14(3):343–50.
115. Fittipaldi A, Ferrari A, Zoppe M, Arcangeli C, Pellegrini V, Beltram F, et al. Cell membrane lipid rafts mediate caveolar endocytosis of HIV-1 Tat fusion proteins. J Biol Chem. 2003;278(36):34141–9.
116. Kaplan IM, Wadia JS, Dowdy SF. Cationic TAT peptide transduction domain enters cells by macropinocytosis. J Control Release. 2005;102(1):247–53.
117. Nakase I, Niwa M, Takeuchi T, Sonomura K, Kawabata N, Koike Y, et al. Cellular uptake of arginine-rich peptides: roles for macropinocytosis and actin rearrangement. Mol Ther. 2004;10(6):1011–22.
118. Richard JP, Melikov K, Brooks H, Prevot P, Lebleu B, Chernomordik LV. Cellular uptake of unconjugated TAT peptide involves clathrin-dependent endocytosis and heparan sulfate receptors. J Biol Chem. 2005;280(15):15300–6.
119. Vandenbroucke RE, De Smedt SC, Demeester J, Sanders NN. Cellular entry pathway and gene transfer capacity of TAT-modified lipoplexes. Biochim Biophys Acta. 2007;1768(3):571–9.
120. Duchardt F, Fotin-Mleczek M, Schwarz H, Fischer R, Brock R. A comprehensive model for the cellular uptake of cationic cell-penetrating peptides. Traffic. 2007;8(7):848–66.
121. Josephson L, Tung CH, Moore A, Weissleder R. High-efficiency intracellular magnetic labeling with novel superparamagnetic-Tat peptide conjugates. Bioconjug Chem. 1999;10(2):186–91.
122. Pasqualini R, Koivunen E, Ruoslahti E. Alpha v integrins as receptors for tumor targeting by circulating ligands. Nat Biotechnol. 1997;15(6):542–6.
123. Gabathuler R. Approaches to transport therapeutic drugs across the blood-brain barrier to treat brain diseases. Neurobiol Dis. 2010;37(1):48–57.
124. Thomas FC, Taskar K, Rudraraju V, Goda S, Thorsheim HR, Gaasch JA, et al. Uptake of ANG1005, a novel paclitaxel derivative, through the blood-brain barrier into brain and experimental brain metastases of breast cancer. Pharm Res. 2009;26(11):2486–94.
125. Gumbleton M, Audus KL. Progress and limitations in the use of *in vitro* cell cultures to serve as a permeability screen for the blood-brain barrier. J Pharm Sci. 2001;90(11):1681–98.
126. Deli MA, Abraham CS, Kataoka Y, Niwa M. Permeability studies on *in vitro* blood-brain barrier models: physiology, pathology, and pharmacology. Cell Mol Neurobiol. 2005;25(1):59–127.
127. Nakagawa S, Deli MA, Kawaguchi H, Shimizudani T, Shimono T, Kittel A, et al. A new blood-brain barrier model using primary rat brain endothelial cells, pericytes and astrocytes. Neurochem Int. 2009;54(3–4):253–63.
128. Naik P, Cucullo L. *In vitro* blood-brain barrier models: current and perspective technologies. J Pharm Sci. 2012;101(4):1337–54.
129. Burek M, Salvador E, Forster CY. Generation of an immortalized murine brain microvascular endothelial cell line as an *in vitro* blood brain barrier model. J Vis Exp. 2012;66:e4022.
130. Weksler BB, Subileau EA, Perriere N, Charneau P, Holloway K, Leveque M, et al. Blood-brain barrier-specific properties of a human adult brain endothelial cell line. FASEB J. 2005;19(13):1872–4.
131. Watson PM, Paterson JC, Thom G, Ginman U, Lundquist S, Webster CI. Modelling the endothelial blood-CNS barriers: a method for the production of robust *in vitro* models of the rat blood-brain barrier and blood-spinal cord barrier. BMC Neurosci. 2013;14:59.

132. Bernas MJ, Cardoso FL, Daley SK, Weinand ME, Campos AR, Ferreira AJ, et al. Establishment of primary cultures of human brain microvascular endothelial cells to provide an *in vitro* cellular model of the blood-brain barrier. Nat Protoc. 2010;5(7):1265–72.
133. Patabendige A, Skinner RA, Abbott NJ. Establishment of a simplified *in vitro* porcine blood-brain barrier model with high transendothelial electrical resistance. Brain Res. 2013;1521:1–15.
134. Garcia-Garcia E, Gil S, Andrieux K, Desmaele D, Nicolas V, Taran F, et al. A relevant *in vitro* rat model for the evaluation of blood-brain barrier translocation of nanoparticles. Cell Mol Life Sci. 2005;62(12):1400–8.
135. Calvo P, Gouritin B, Chacun H, Desmaele D, D'Angelo J, Noel JP, et al. Long-circulating PEGylated polycyanoacrylate nanoparticles as new drug carrier for brain delivery. Pharm Res. 2001;18(8): 1157–66.
136. Kim HR, Andrieux K, Gil S, Taverna M, Chacun H, Desmaele D, et al. Translocation of poly(ethylene glycol-co-hexadecyl)cyanoacrylate nanoparticles into rat brain endothelial cells: role of apolipoproteins in receptor-mediated endocytosis. Biomacromolecules. 2007;8(3):793–9.
137. Kim HR, Gil S, Andrieux K, Nicolas V, Appel M, Chacun H, et al. Low-density lipoprotein receptor-mediated endocytosis of PEGylated nanoparticles in rat brain endothelial cells. Cell Mol Life Sci. 2007;64(3):356–64.
138. Hornok V, Bujdoso T, Toldi J, Nagy K, Demeter I, Fazakas C, et al. Preparation and properties of nanoscale containers for biomedical application in drug delivery: preliminary studies with kynurenic acid. J Neural Transm. 2012;119(2):115–21.
139. Tian W, Ying X, Du J, Guo J, Men Y, Zhang Y, et al. Enhanced efficacy of functionalized epirubicin liposomes in treating brain glioma-bearing rats. Eur J Pharm Sci. 2010;41(2):232–43.
140. Liu Y, Huang R, Han L, Ke W, Shao K, Ye L, et al. Brain-targeting gene delivery and cellular internalization mechanisms for modified rabies virus glycoprotein RVG29 nanoparticles. Biomaterials. 2009;30(25):4195–202.
141. Xie Y, Ye L, Zhang X, Cui W, Lou J, Nagai T, et al. Transport of nerve growth factor encapsulated into liposomes across the blood-brain barrier: *in vitro* and *in vivo* studies. J Control Release. 2005;105(1–2):106–19.
142. Gil ES, Li J, Xiao H, Lowe TL. Quaternary ammonium beta-cyclodextrin nanoparticles for enhancing doxorubicin permeability across the *in vitro* blood-brain barrier. Biomacromolecules. 2009;10(3):505–16.
143. Prades R, Guerrero S, Araya E, Molina C, Salas E, Zurita E, et al. Delivery of gold nanoparticles to the brain by conjugation with a peptide that recognizes the transferrin receptor. Biomaterials. 2012;33(29):7194–205.
144. Gaillard PJ, Voorwinden LH, Nielsen JL, Ivanov A, Atsumi R, Engman H, et al. Establishment and functional characterization of an *in vitro* model of the blood-brain barrier, comprising a co-culture of brain capillary endothelial cells and astrocytes. Eur J Pharm Sci. 2001;12(3):215–22.
145. Agyare EK, Curran GL, Ramakrishnan M, Yu CC, Poduslo JF, Kandimalla KK. Development of a smart nano-vehicle to target cerebrovascular amyloid deposits and brain parenchymal plaques observed in Alzheimer's disease and cerebral amyloid angiopathy. Pharm Res. 2008;25(11):2674–84.
146. Franke H, Galla H, Beuckmann CT. Primary cultures of brain microvessel endothelial cells: a valid and flexible model to study drug transport through the blood-brain barrier *in vitro*. Brain Res Brain Res Protocol. 2000;5(3):248–56.
147. Walters EM, Agca Y, Ganjam V, Evans T. Animal models got you puzzled?: Think pig. Ann N Y Acad Sci. 2011;1245:63–4.
148. Smith M, Omidi Y, Gumbleton M. Primary porcine brain microvascular endothelial cells: biochemical and functional characterisation as a model for drug transport and targeting. J Drug Target. 2007;15(4):253–68.
149. Lind NM, Moustgaard A, Jelsing J, Vajta G, Cumming P, Hansen AK. The use of pigs in neuroscience: modeling brain disorders. Neurosci Biobehav Rev. 2007;31(5):728–51.
150. Luo YL, Lin L, Bolund L, Jensen TG, Sorensen CB. Genetically modified pigs for biomedical research. J Inherit Metab Dis. 2012;35(4):695–713.
151. Wagner S, Kufleitner J, Zensi A, Dadparvar M, Wien S, Bungert J, et al. Nanoparticulate transport of oximes over an *in vitro* blood-brain barrier model. PLoS ONE. 2010;5(12):e14213.
152. Qiao R, Jia Q, Huwel S, Xia R, Liu T, Gao F, et al. Receptor-mediated delivery of magnetic nanoparticles across the blood-brain barrier. ACS Nano. 2012;6(4):3304–10.
153. Kuo YC, Ko HF. Targeting delivery of saquinavir to the brain using 83–14 monoclonal antibody-grafted solid lipid nanoparticles. Biomaterials. 2013;34(20):4818–30.
154. Kuo YC, Shih-Huang CY. Solid lipid nanoparticles carrying chemotherapeutic drug across the blood-brain barrier through insulin receptor-mediated pathway. J Drug Target. 2013;21(8):730–8.
155. Jensen SA, Day ES, Ko CH, Hurley LA, Luciano JP, Kouri FM, et al. Spherical nucleic acid nanoparticle conjugates as an RNAi-based therapy for glioblastoma. Sci Transl Med. 2013;5(209): 209ra152.
156. Williams RL, Risau W, Zerwes H-G, Drexler H, Aguzzi A, Wagner EF. Endothelioma cells expressing the polyoma middle T oncogene induce hemangiomas by host cell recruitment. Cell. 1989;57(6): 1053–63.
157. Omidi Y, Campbell L, Barar J, Connell D, Akhtar S, Gumbleton M. Evaluation of the immortalised mouse brain capillary endothelial cell line, b.End3, as an *in vitro* blood-brain barrier model for drug uptake and transport studies. Brain Res. 2003;990(1–2):95–112.
158. Omidi Y, Barar J, Ahmadian S, Heidari HR, Gumbleton M. Characterization and astrocytic modulation of system L transporters in brain microvasculature endothelial cells. Cell Biochem Funct. 2008;26(3):381–91.
159. Wagner S, Zensi A, Wien SL, Tschickardt SE, Maier W, Vogel T, et al. Uptake mechanism of ApoE-modified nanoparticles on brain capillary endothelial cells as a blood-brain barrier model. PLoS ONE. 2012;7(3):e32568.
160. Yuan W, Li G, Gil ES, Lowe TL, Fu BM. Effect of surface charge of immortalized mouse cerebral endothelial cell monolayer on transport of charged solutes. Ann Biomed Eng. 2010;38(4):1463–72.
161. Brown RC, Morris AP, O'Neil RG. Tight junction protein expression and barrier properties of immortalized mouse brain microvessel endothelial cells. Brain Res. 2007;1130(1):17–30.
162. Markoutsa E, Pampalakis G, Niarakis A, Romero IA, Weksler B, Couraud PO, et al. Uptake and permeability studies of BBB-targeting immunoliposomes using the hCMEC/D3 cell line. Eur J Pharm Biopharm. 2011;77(2):265–74.
163. Salvati E, Re F, Sesana S, Cambianica I, Sancini G, Masserini M, et al. Liposomes functionalized to overcome the blood-brain barrier and to target amyloid-beta peptide: the chemical design affects the permeability across an *in vitro* model. Int J Nanomedicine. 2013;8: 1749–58.
164. Ragnaill MN, Brown M, Ye D, Bramini M, Callanan S, Lynch I, et al. Internal benchmarking of a human blood-brain barrier cell model for screening of nanoparticle uptake and transcytosis. Eur J Pharm Biopharm. 2011;77(3):360–7.
165. Dan M, Cochran DB, Yokel RA, Dziubla TD. Binding, transcytosis and biodistribution of anti-PECAM-1 iron oxide nanoparticles for brain-targeted delivery. PLoS ONE. 2013;8(11):e81051.
166. Georgieva JV, Brinkhuis RP, Stojanov K, Weijers CA, Zuilhof H, Rutjes FP, et al. Peptide-mediated blood-brain barrier transport of polymersomes. Angew Chem Int Ed Engl. 2012;51(33):8339–42.
167. Stojanov K, Georgieva JV, Brinkhuis RP, van Hest JC, Rutjes FP, Dierckx RA, et al. *In vivo* biodistribution of prion- and GM1-

targeted polymersomes following intravenous administration in mice. Mol Pharm. 2012;9(6):1620–7.
168. Chattopadhyay N, Zastre J, Wong HL, Wu XY, Bendayan R. Solid lipid nanoparticles enhance the delivery of the HIV protease inhibitor, atazanavir, by a human brain endothelial cell line. Pharm Res. 2008;25(10):2262–71.
169. Lippmann ES, Azarin SM, Kay JE, Nessler RA, Wilson HK, Al-Ahmad A, et al. Derivation of blood-brain barrier endothelial cells from human pluripotent stem cells. Nat Biotechnol. 2012;30(8):783–91.
170. Lippmann ES, Al-Ahmad A, Azarin SM, Palecek SP, Shusta EV. A retinoic acid-enhanced, multicellular human blood-brain barrier model derived from stem cell sources. Sci Rep. 2014;4:4160.
171. Hellinger E, Veszelka S, Toth AE, Walter F, Kittel A, Bakk ML, et al. Comparison of brain capillary endothelial cell-based and epithelial (MDCK-MDR1, Caco-2, and VB-Caco-2) cell-based surrogate blood-brain barrier penetration models. Eur J Pharm Biopharm. 2012;82(2):340–51.
172. Zhao S, Dai W, He B, Wang J, He Z, Zhang X, et al. Monitoring the transport of polymeric micelles across MDCK cell monolayer and exploring related mechanisms. J Control Release. 2012;158(3):413–23.
173. Kirby BP, Pabari R, Chen CN, Al Baharna M, Walsh J, Ramtoola Z. Comparative evaluation of the degree of pegylation of poly(lactic-co-glycolic acid) nanoparticles in enhancing central nervous system delivery of loperamide. J Pharm Pharmacol. 2013;65(10):1473–81.
174. Cucullo L, Hossain M, Puvenna V, Marchi N, Janigro D. The role of shear stress in blood-brain barrier endothelial physiology. BMC Neurosci. 2011;12:40.
175. Booth R, Kim H. Characterization of a microfluidic *in vitro* model of the blood-brain barrier (muBBB). Lab Chip. 2012;12(10):1784–92.
176. European Directorate for the Quality of Medicines and Healthcare. Alternatives to Animal Testing. Available from: https://www.edqm.eu/en/Alternatives-to-animal-testing-1483.html.
177. Palmer AM, Alavijeh MS. Translational CNS medicines research. Drug Discov Today. 2012;17(19–20):1068–78.
178. Desai N. Challenges in development of nanoparticle-based therapeutics. AAPS J. 2012;14(2):282–95.
179. El-Ansary A, Al-Daihan S. On the toxicity of therapeutically used nanoparticles: an overview. J Toxicol. 2009;2009.
180. Sahay G, Alakhova DY, Kabanov AV. Endocytosis of nanomedicines. J Control Release. 2010;145(3):182–95.
181. Trickler WJ, Lantz SM, Murdock RC, Schrand AM, Robinson BL, Newport GD, et al. Brain microvessel endothelial cells responses to gold nanoparticles: *in vitro* pro-inflammatory mediators and permeability. Nanotoxicology. 2011;5(4):479–92.
182. Ye D, Raghnaill MN, Bramini M, Mahon E, Aberg C, Salvati A, et al. Nanoparticle accumulation and transcytosis in brain endothelial cell layers. Nanoscale. 2013;5(22):11153–65.
183. Frigell J, Garcia I, Gomez-Vallejo V, Llop J, Penades S. 68Ga-labeled gold glyconanoparticles for exploring blood-brain barrier permeability: preparation, biodistribution studies, and improved brain uptake via neuropeptide conjugation. J Am Chem Soc. 2014;136(1):449–57.
184. Ebrahimi Shahmabadi H, Movahedi F, Koohi Moftakhari Esfahani M, Alavi SE, Eslamifar A, Mohammadi Anaraki G *et al*. Efficacy of Cisplatin-loaded polybutyl cyanoacrylate nanoparticles on the glioblastoma. Tumour Biol. 2014.
185. Ambruosi A, Yamamoto H, Kreuter J. Body distribution of polysorbate-80 and doxorubicin-loaded [14C]poly(butyl cyanoacrylate) nanoparticles after i.v. administration in rats. J Drug Target. 2005;13(10):535–42.
186. Kuo YC, Chung CY. Transcytosis of CRM197-grafted polybutylcyanoacrylate nanoparticles for delivering zidovudine across human brain-microvascular endothelial cells. Colloids Surf B: Biointerfaces. 2012;91:242–9.
187. Meister S, Zlatev I, Stab J, Docter D, Baches S, Stauber RH, et al. Nanoparticulate flurbiprofen reduces amyloid-beta42 generation in an *in vitro* blood-brain barrier model. Alzheimers Res Ther. 2013;5(6):51.
188. Chen YC, Hsieh WY, Lee WF, Zeng DT. Effects of surface modification of PLGA-PEG-PLGA nanoparticles on loperamide delivery efficiency across the blood-brain barrier. J Biomater Appl. 2013;27(7):909–22.
189. Chang J, Paillard A, Passirani C, Morille M, Benoit JP, Betbeder D, et al. Transferrin adsorption onto PLGA nanoparticles governs their interaction with biological systems from blood circulation to brain cancer cells. Pharm Res. 2012;29(6):1495–505.
190. Costantino L, Gandolfi F, Tosi G, Rivasi F, Vandelli MA, Forni F. Peptide-derivatized biodegradable nanoparticles able to cross the blood-brain barrier. J Control Release. 2005;108(1):84–96.
191. Costantino L, Gandolfi F, Bossy-Nobs L, Tosi G, Gurny R, Rivasi F, et al. Nanoparticulate drug carriers based on hybrid poly(D, L-lactide-co-glycolide)-dendron structures. Biomaterials. 2006;27(26):4635–45.
192. Jiang X, Xin H, Ren Q, Gu J, Zhu L, Du F, et al. Nanoparticles of 2-deoxy-D-glucose functionalized poly(ethylene glycol)-co-poly(trimethylene carbonate) for dual-targeted drug delivery in glioma treatment. Biomaterials. 2014;35(1):518–29.
193. An S, Kuang Y, Shen T, Li J, Ma H, Guo Y, et al. Brain-targeting delivery for RNAi neuroprotection against cerebral ischemia reperfusion injury. Biomaterials. 2013;34(35):8949–59.
194. Kratzer I, Wernig K, Panzenboeck U, Bernhart E, Reicher H, Wronski R, et al. Apolipoprotein A-I coating of protamine-oligonucleotide nanoparticles increases particle uptake and transcytosis in an *in vitro* model of the blood-brain barrier. J Control Release. 2007;117(3):301–11.
195. Chaturvedi M, Molino Y, Sreedhar B, Khrestchatisky M, Kaczmarek L. Tissue inhibitor of matrix metalloproteinases-1 loaded poly(lactic-co-glycolic acid) nanoparticles for delivery across the blood-brain barrier. Int J Nanomedicine. 2014;9:575–88.
196. Gao H, Yang Z, Zhang S, Pang Z, Liu Q, Jiang X. Study and evaluation of mechanisms of dual targeting drug delivery system with tumor microenvironment assays compared with normal assays. Acta Biomater. 2014;10(2):858–67.
197. Hemmer R, Hall A, Spaulding R, Rossow B, Hester M, Caroway M, et al. Analysis of biotinylated generation 4 poly(amidoamine) (PAMAM) dendrimer distribution in the rat brain and toxicity in a cellular model of the blood-brain barrier. Molecules. 2013;18(9):11537–52.
198. Du J, Lu WL, Ying X, Liu Y, Du P, Tian W, et al. Dual-targeting topotecan liposomes modified with tamoxifen and wheat germ agglutinin significantly improve drug transport across the blood-brain barrier and survival of brain tumor-bearing animals. Mol Pharm. 2009;6(3):905–17.
199. Qin Y, Fan W, Chen H, Yao N, Tang W, Tang J, et al. *In vitro* and *in vivo* investigation of glucose-mediated brain-targeting liposomes. J Drug Target. 2010;18(7):536–49.
200. Ying X, Wen H, Lu WL, Du J, Guo J, Tian W, et al. Dual-targeting daunorubicin liposomes improve the therapeutic efficacy of brain glioma in animals. J Control Release. 2010;141(2):183–92.
201. Ding H, Sagar V, Agudelo M, Pilakka-Kanthikeel S, Atluri VS, Raymond A, et al. Enhanced blood-brain barrier transmigration using a novel transferrin embedded fluorescent magneto-liposome nanoformulation. Nanotechnology. 2014;25(5):055101.
202. Markoutsa E, Papadia K, Clemente C, Flores O, Antimisiaris SG. Anti-Abeta-MAb and dually decorated nanoliposomes: effect of Abeta1-42 peptides on interaction with hCMEC/D3 cells. Eur J Pharm Biopharm. 2012;81(1):49–56.
203. Re F, Cambianica I, Zona C, Sesana S, Gregori M, Rigolio R, et al. Functionalization of liposomes with ApoE-derived peptides at

different density affects cellular uptake and drug transport across a blood-brain barrier model. Nanomedicine. 2011;7(5):551–9.
204. Brun E, Carriere M, Mabondzo A. *In vitro* evidence of dysregulation of blood-brain barrier function after acute and repeated/long-term exposure to TiO(2) nanoparticles. Biomaterials. 2012;33(3):886–96.
205. Thomsen LB, Linemann T, Pondman KM, Lichota J, Kim KS, Pieters RJ, et al. Uptake and transport of superparamagnetic iron oxide nanoparticles through human brain capillary endothelial cells. ACS Chem Neurosci. 2013;4(10):1352–60.
206. Liu D, Lin B, Shao W, Zhu Z, Ji T, Yang C. *In vitro* and *in vivo* studies on the transport of PEGylated silica nanoparticles across the blood-brain barrier. ACS Appl Mater Interfaces. 2014;6(3):2131–6.
207. Hanada S, Fujioka K, Inoue Y, Kanaya F, Manome Y, Yamamoto K. Cell-based *in vitro* blood-brain barrier model can rapidly evaluate nanoparticles' brain permeability in association with particle size and surface modification. Int J Mol Sci. 2014;15(2):1812–25.
208. Dadparvar M, Wagner S, Wien S, Kufleitner J, Worek F, von Briesen H, et al. HI 6 human serum albumin nanoparticles—development and transport over an *in vitro* blood-brain barrier model. Toxicol Lett. 2011;206(1):60–6.
209. Pilakka-Kanthikeel S, Atluri VS, Sagar V, Saxena SK, Nair M. Targeted brain derived neurotropic factors (BDNF) delivery across the blood-brain barrier for neuro-protection using magnetic nano carriers: an *in-vitro* study. PLoS ONE. 2013;8(4):e62241.
210. Kuo YC, Lee CL. Methylmethacrylate-sulfopropylmethacrylate nanoparticles with surface RMP-7 for targeting delivery of antiretroviral drugs across the blood-brain barrier. Colloids Surf B: Biointerfaces. 2012;90:75–82.
211. Ren J, Shen S, Wang D, Xi Z, Guo L, Pang Z, et al. The targeted delivery of anticancer drugs to brain glioma by PEGylated oxidized multi-walled carbon nanotubes modified with angiopep-2. Biomaterials. 2012;33(11):3324–33.
212. Lu W, Zhang Y, Tan YZ, Hu KL, Jiang XG, Fu SK. Cationic albumin-conjugated pegylated nanoparticles as novel drug carrier for brain delivery. J Control Release. 2005;107(3):428–48.
213. Abbott NJ, Dolman DE, Drndarski S, Fredriksson SM. An improved *in vitro* blood-brain barrier model: rat brain endothelial cells co-cultured with astrocytes. Methods Mol Biol. 2012;814:415–30.
214. Huang R, Ke W, Han L, Liu Y, Shao K, Ye L, et al. Brain-targeting mechanisms of lactoferrin-modified DNA-loaded nanoparticles. J Cereb Blood Flow Metab. 2009;29(12):1914–23.
215. Patabendige A, Skinner RA, Morgan L, Abbott NJ. A detailed method for preparation of a functional and flexible blood-brain barrier model using porcine brain endothelial cells. Brain Res. 2013;1521:16–30.
216. Lockman PR, Koziara J, Roder KE, Paulson J, Abbruscato TJ, Mumper RJ, et al. *In vivo* and *in vitro* assessment of baseline blood-brain barrier parameters in the presence of novel nanoparticles. Pharm Res. 2003;20(5):705–13.
217. Chang J, Jallouli Y, Kroubi M, Yuan XB, Feng W, Kang CS, et al. Characterization of endocytosis of transferrin-coated PLGA nanoparticles by the blood-brain barrier. Int J Pharm. 2009;379(2):285–92.
218. Kreuter J, Ramge P, Petrov V, Hamm S, Gelperina SE, Engelhardt B, et al. Direct evidence that polysorbate-80-coated poly(butylcyanoacrylate) nanoparticles deliver drugs to the CNS via specific mechanisms requiring prior binding of drug to the nanoparticles. Pharm Res. 2003;20(3):409–16.